THE MINERALOGICAL MAGAZINE

AND

JOURNAL OF
THE MINERALOGICAL SOCIETY

No. 228 March, 1955 Vol. XXX

Transitional optics of some andesines and labradorites.

By I. D. Muir, B.A., Ph.D., F.G.S.

Department of Mineralogy and Petrology, University of Cambridge.

[Read March 25, 1954.]

I. Introduction.

RECENT optical and structural investigations have shown that both high- and low-temperature forms of plagioclase can exist naturally over the range An_{0-70}, and in the more basic plagioclases (An_{70-90}) Gay (1954) has shown that a structural distinction can be effected although no definite optical differences have yet been established. In the anorthite range slight optical and distinct structural differences have been observed between synthetic plagioclases and crystal lapilli on the one hand and all other natural plagioclases on the other (Gay, 1953).

Nearly all published data on natural high-temperature plagioclases are confined to volcanic rocks and almost without exception published information on plutonic or metamorphic rocks indicates a low-temperature state for the plagioclase. No systematic investigation of the plagioclases from hypabyssal rocks or from the smaller plutonic intrusions appears to have been undertaken; and the current views of most optical workers seem to indicate that plagioclase felspars belong either to the high- or the low-temperature series, and that transitional states, if present at all, are very rare. The only specific records of transitional optics in plagioclases are in the works of Oftedahl (1948) on the andesines of the rhomb-porphyries in the Oslo area and of Tuttle and Keith (1954) for the oligoclase (An_{17}) of the Beinn an Dubhaich granite, Skye.

In this paper all the plagioclases studied are andesines or labradorites and most of them come from the great tholeiitic dolerite sills in which many of the parent rocks are truly gabbroic in texture. All the specimens have been examined optically using a Leitz four-axis universal stage, and refractive index measurements were carried out on four of the specimens selected for analysis. X-ray single-crystal oscillation photographs have also been taken of most of them in their natural state. Selected grains were heat-treated and then examined optically again, and in critical cases a further X-ray examination has been made of the heat-treated crystals.

II. The recognition of high- and low-temperature optics.

Köhler (1941) was the first to note definitely the effect of the thermal history on the optics of plagioclase felspars. He showed that plagioclases occurring as phenocrysts in volcanic rocks had an optical orientation which differed noticeably from that of the 'standard plagioclases' of plutonic rocks or gneisses on which Reinhard (1931) had based his determinative curves. Köhler's investigations covered the composition range An_{35-73}, and as standard high-temperature plagioclases he selected for further optical study fragments from three of the analysed fractions of felspars having compositions 35·5, 45·5, and 54 % An, described by Ernst and Nieland (1934) from the island of Linosa.

In the andesine-labradorite range the distinction between high- and low-temperature forms can best be shown optically by the positions of the (010) or (001) face poles when plotted on a stereogram with fixed optical directions (fig. 1). For plagioclases more sodic than 45 % An the distinction is greater if the positions of the two optic axes A and B are used and plotted on a conventionally oriented stereogram with (001) at the centre and (010) at the right-hand horizontal radius (fig. 2).

The measurements were carried out using white light except for the final setting of the optic axial plane and for this a yellow 589 $\mu\mu$ filter was used to minimize the effect of the pronounced dispersion. In all specimens, except those from Linosa, St. John's Point, and Esterel, at least ten separate twinned crystals were measured using the orthoscopic method. Since large simply-twinned fragments of the Linosa, St. John's Point, and Esterel felspars were available, these were mounted, ground flat on the upper surface, and oriented using the conoscopic method. Because of the pronounced dispersion of the optic axial plane

in plagioclases a conoscopic setting of this plane is not as satisfactory as the orthoscopic setting, but the conoscopic method can detect the positions of the optic axes to $\pm\frac{1}{2}°$ which is a considerable improvement on the accuracy of the conventional orthoscopic method.

A striking feature of all the rocks examined containing plagioclase An_{35-50} was the number of individual crystals (about 5–10 % of the total) elongated parallel to the x crystallographic axis. Sections of such crystals oriented perpendicular to the x-axis are readily recognized in thin section by their square cross-sections and by the presence of the (001) and (010) cleavages. Moreover, in such crystals simple fourlings with re-entrant angles of 8° developed by primary twinning on the albite and Ala-A laws can frequently be observed and such sections are particularly suitable for making accurate optical measurements. Primary twinning of this type on the Ala-A law seems to be associated with plagioclase whose composition centres around An_{40}. Plagioclases more basic than An_{50} were examined carefully to see whether similar fourlings or simple Ala-A twins were developed, but none could be found.

By using twinned fourlings of this type it was possible to locate the position of the x crystallographic axis and the (010) plane very accurately, and, since for all plagioclases the crystallographic β-angle does not deviate by more than $\frac{1}{2}°$ from 116°, [001] can also be located accurately when the optical orientation has been established. In many of these primary twins the sharp albite composition plane proved to be vicinal in nature, being inclined to the true (010) plane by as much as 3°. Such deviations were never observed for twins on (001). All plotted points in the diagrams represent mean angular values measured over twin axes, twin axes being used in all cases as reference directions.

Refractive index measurements of the very few analysed high-temperature and transitional plagioclase felspars available approach very closely to Chayes's curves (1952), and it would appear that any clear distinction in the refractive indices of the high- and low-temperature series of plagioclases can only be effected at compositions approaching pure albite. The only systematic deviation from Chayes's curves that could be noted was a tendency for the refractive indices of high-temperature and transitional plagioclases more sodic than about An_{50} to be about 0·001 lower than the curves (with the exception of pure albite), and for those more basic than An_{50} to be higher by about the same amount. These deviations are within the limits of experimental error and will not be considered further as the data at present are so meagre. It would seem, therefore, that with the exception of very sodic

plagioclases, any estimation of the composition of a natural plagioclase felspar based on accurate refractive index measurements should be satisfactory within $\pm 2\,\%$, irrespective of the structural state of the mineral.

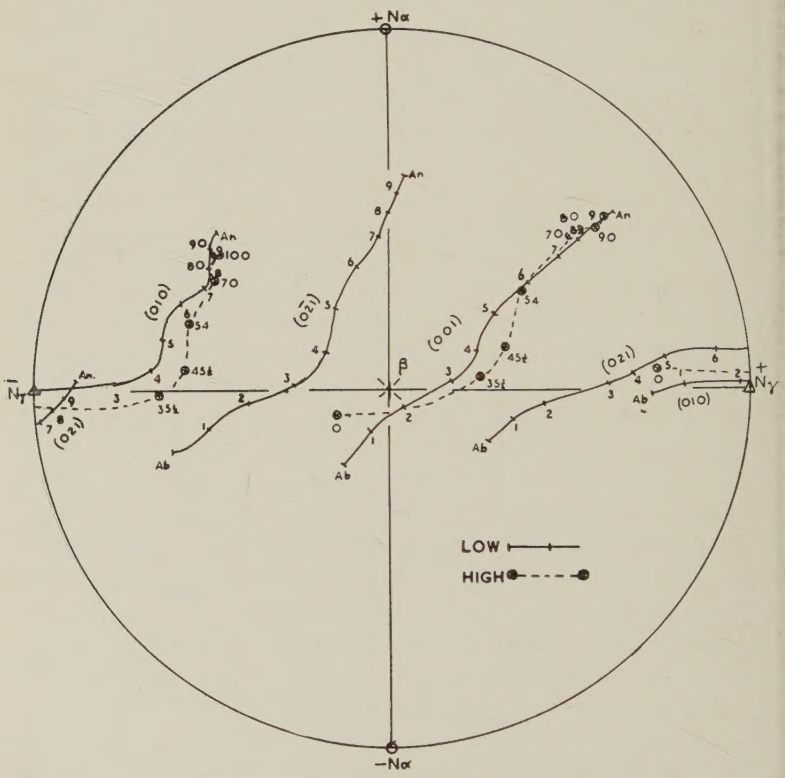

Fig. 1. Fedorov-Nikitin type stereogram showing the migration of crystallographic poles for high- and low-temperature plagioclase felspars with reference to fixed optical vectors. Low-temperature curves of Reinhard (1931); high-temperature curves based on Tuttle and Bowen (1950), Köhler (1941), and Tertsch (1942).

III. The structures of the intermediate plagioclases.

In the low-temperature intermediate plagioclases, An_{30-70}, X-ray reflections which have '$h+k$' even and 'l' odd (indexed on the basis of a 14 Å. c-axis) are doubled. These doubled spots, corresponding to the type 'b' reflections of anorthite described by Gay (1954), are symmetrically disposed about the positions of the odd-layer lines on c-axis

oscillation photographs and symmetrically about all layer lines for a- and b-axis photographs. Cole, Sörum, and Taylor (1951) showed that the separation of these doubled spots varied in a regular manner and could be correlated with the composition of the felspar. In the low-temperature

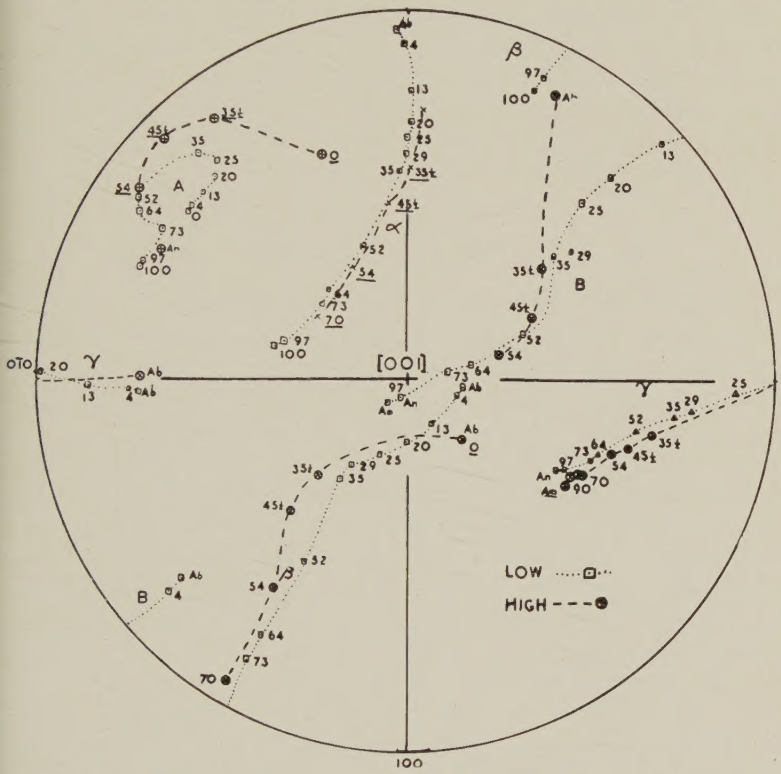

FIG. 2. Stereogram showing the positions of the poles of the principal vibration directions and of the optic axes of high- and low-temperature plagioclase felspars. Low-temperature curves of Reinhard (1931); high-temperature curves based on Tuttle and Bowen (1950), Köhler (1941), and Tertsch (1942).

plagioclases in the range An_{40-55} the subsidiary type 'b' reflections although weak do not seem to vary noticeably in intensity with change of composition. More recently, Gay (1954) has shown that these weak reflections can be made to disappear by suitable heat-treatment leaving a structure with a 7 Å. c-axis, and that in the high-temperature state a 7 Å. c-axis type of felspar can exist over the whole range from albite to about An_{90}.

Buerger (1948) and Laves (1952) have suggested that the transformations between high- and low-temperature forms in felspars are order-disorder effects; Gay (1954) considers that this suggestion is in agreement with the nature of the changes observed when basic plagioclases are heated, and that there is little doubt that inversions of this kind exist over the whole of the plagioclase system. He states, further, that by the very nature of the inversion, felspars in transitional states can exist quite stably throughout the series, and has demonstrated their existence for basic plagioclases. In the alkali-felspars, transitional types are now known (Tuttle and Keith, 1954).

IV. Specimens examined.

The specimens to be investigated were selected carefully so that the compositions of the respective plagioclases and pyroxenes in the different doleritic rocks were as similar as possible. In this way it was hoped that any relation between exsolution and inversion in the pyroxenes and the structural state of the plagioclase would become evident. For felspars in the andesine–sodic-labradorite range this has involved a study more particularly of the iron-rich differentiates. The plagioclase from the iron-rich facies of the Beaver Bay diabase has been described in detail, and textural features of the other plagioclases examined have been compared with those noted in this mineral. Mean values for the positions of the optic axes of all felspars examined are given as Becke co-ordinates in table I.

(i) *Andesine from the Beaver Bay diabase, Minnesota.*

This plagioclase comes from a specimen of the relatively coarse-grained iron-rich facies of the great pre-Cambrian Beaver Bay sill-like diabase intrusion (Grout and Schwartz, 1939). The principal associated minerals of the plagioclase are olivine (Fa_{80}), ferroaugite ($Ca_{38}Mg_{28}Fe_{34}$) with extremely fine exsolution lamellae, pigeonite ($Ca_9Mg_{27}Fe_{64}$) much of which has inverted to orthopyroxene, and interstitial primary orthopyroxene (Of_{75}). The pyroxene relations have already been described in detail (Muir, 1954).

The tabular subhedral plagioclase crystals An_{44}, which average about two millimetres in length, are very fresh and virtually unzoned, except at the margins where strong zoning to about An_{20} may occur. Most of the crystals are elongated parallel to the z crystallographic axis, and are flattened on (010), but about ten per cent. of the individuals are elong-

TABLE I. Optical data of plagioclases.

Average values for the positions of optic axes A and B in the projection on (001) of plagioclases (Becke co-ordinates).

Plagioclase.	Composition Wt. % An.	A. λ.	A. ϕ.	B. λ.	B. ϕ.	$2V_\gamma$.
Esterel...	40	+80½°	−43°	+35½°	+38°	90°
Beaver Bay	44	+80½	−44½	+30½	+37½	86
New Amalfi EH52...	46½	+80½	−50	+20	+35½	79½
New Amalfi EH20...	50½	+78½	−54	+14	+33	77½
New Amalfi	55	+75	−77	+8	+28	78½
Mount Wellington (summit)	56	+74	−54	+7	+27	81
St. John's Point ...	62	+74	−56	+6½	+25	81
Mount Wellington (875 feet)	68	+68½	−56½	+2	+20½	85½

Albite twins, angles to (010).

	α.	β.	γ.
Esterel	88°	66°	24½°
Beaver Bay	85	64	26
New Amalfi EH52	83½	64	27
New Amalfi EH20	78	63½	29½
New Amalfi	73	64½	31½
Mount Wellington (summit)	73	62	33½
St. John's Point	70½	62½	35
Mount Wellington (875 feet)	68½	61	37

Albite twins, heated to 1000° C. for 72 hours. (Average values for two twinned crystals.)

	α.	β.	γ.	$2V_\gamma$.
Esterel	88½°	64°	26½°	88°
Beaver Bay ...	86	61½	29	85
New Amalfi EH52	83½	59½	31½	78
New Amalfi EH20	79	60	32	—
New Amalfi ...	74½	61½	33	78
St. John's Point	70½	60	37	77

ated parallel to the x-axis and these show the albite-Ala fourlings described earlier. In such simple doublets or fourlings a feature of the twinning is the presence of only a few almost hair-like subsidiary albite-twin lamellae in the major albite-twinned sub-individuals. A very few extremely fine lamellae parallel to (001) presumably of pericline type are also present. The crystals elongated parallel to the z-axis are generally quite coarsely twinned polysynthetically on the albite law, the average width of the lamellae being about 0·02 mm. Carlsbad and direct albite-Carlsbad twins are also quite frequent, and it is noticeable that here too

the large Carlsbad- and albite-twinned sub-individuals are almost devoid of the fine hair-like subsidiary albite lamellae. The significance of these fine lamellae will be considered again later in this paper.

The optical orientation of this plagioclase is given in figs. 3*a*, 4, and 5 where it can be seen that both the pole of (010) for 12 twinned crystals and the position of optic axis A for 20 crystals lie in a position almost half-way between the standard low- and high-temperature curves.

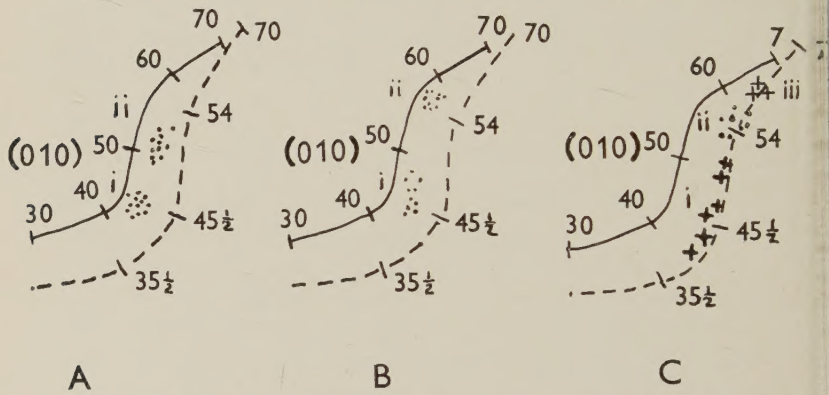

FIG. 3. Migration curves of the (010) pole for high- and low-temperature plagioclase showing the plotted positions of the poles of albite twin axes for the felspars investigated.

A (i) Andesine, from diabase M3174, Beaver Bay, Minnesota.
(ii) Labradorite from quartz-dolerite EH20, New Amalfi, South Africa.

B (i) Andesine from iron-rich quartz-dolerite EH52, New Amalfi.
(ii) Labradorite from augite-hypersthene-dolerite, New Amalfi.

C (i) Andesine, crystal fragments from Monte Rosso, Linosa, Mediterranean.
(ii) Labradorite from dolerite, summit of Mt. Wellington, Tasmania.
(iii) Labradorite from dolerite at height 875 feet, Mt. Wellington, Tasmania.

Unless the composition is known, any inference on the structural state of the felspar based on optic axes B is difficult, owing to the similar trends of the curves.

X-ray oscillation photographs were taken about all three crystallographic axes on one of the large sub-individuals of an albite-Ala fourling which plotted about the centre of the field of scatter. (The remainder of this crystal was used subsequently for refractive index determination and for heat-treatment.) The X-ray photographs showed no subsidiary reflections whatever, indicating that the mineral was structurally in the high-temperature state with a 7 Å. *c*-axis.

As the refractive indices of the Beaver Bay plagioclase would seem to

indicate a composition slightly more basic than that indicated by the (010)-face pole, it seemed possible that variation in potash content or other minor constituents might be responsible for the differences in

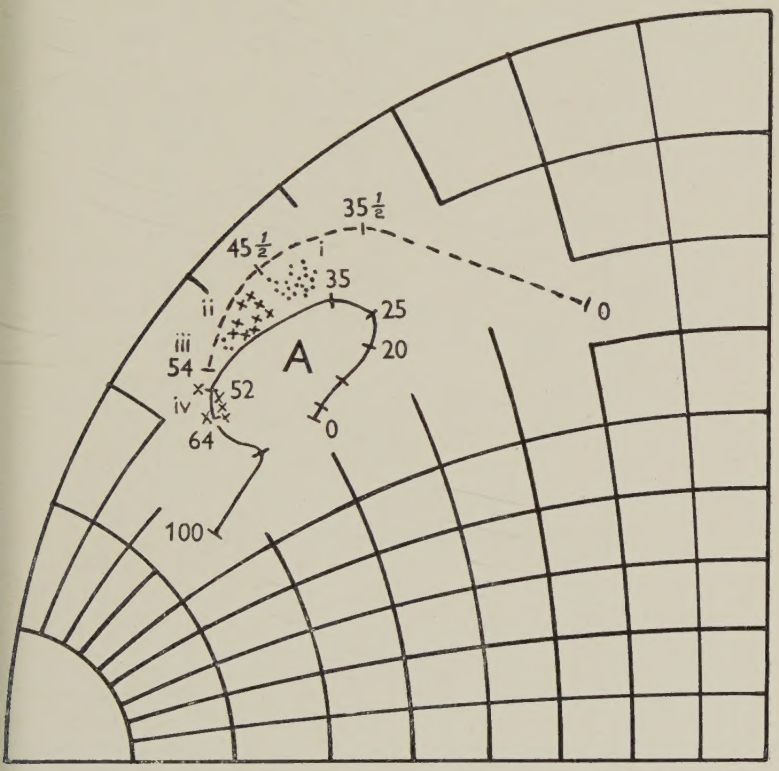

Fig. 4. Poles of optic axis A for analysed felspars.

(i) Andesine from iron-rich diabase M3174, Beaver Bay, Minnesota.
(ii) Andesine from iron-rich quartz-dolerite EH52, New Amalfi, South Africa.
(iii) Labradorite from quartz-dolerite EH20, New Amalfi.
(iv) Labradorite from augite-hypersthene-dolerite, New Amalfi.

optical orientation between this and the standard Linosa felspar $An_{45\cdot5}$. The mineral was therefore separated for chemical analysis using an isodynamic separator and centrifuge, and the final sample was examined carefully to ensure that the zoned marginal portions of the crystals and the felspar of the mesostasis had been removed. The analysis of this felspar together with that of the comparable Linosa andesine are given in columns 1 and A respectively of table II. Comparison of the two

analyses makes it clear that the potash content cannot have had any differential effect on the optical orientation, and this agrees with the conclusions of Chudoba and Engels (1937), but the higher iron content of the Beaver Bay andesine may well be responsible for the exceptionally slight differences in refractive indices of the two minerals. In the

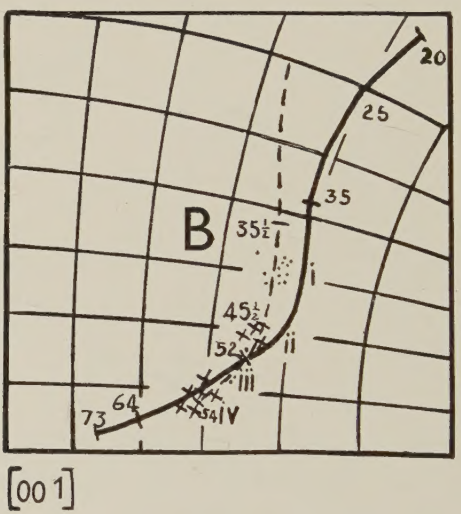

Fig. 5. Poles of optic axis B for analysed felspars.

(i) Andesine from iron-rich diabase M3174, Beaver Bay, Minnesota.
(ii) Andesine from iron-rich quartz-dolerite EH52, New Amalfi, South Africa.
(iii) Labradorite from quartz-dolerite EH20, New Amalfi, South Africa.
(iv) Labradorite from augite-hypersthene-dolerite, New Amalfi, South Africa.

Beaver Bay plagioclase there has been no exsolution of iron in the felspar such as occurs in the comparable more slowly cooled plagioclase in the ferrogabbros of the Skaergaard intrusion (Wager and Deer, 1939).

The remainder of the crystal used for the X-ray investigation and another similar albite-Ala fourling lying near the centre of the field of scatter of the (010) pole were cut out from a thin section and heated in a platinum fusion furnace for 72 hours at 1000° C. and then air cooled. They were then remounted and their optics determined again. The plotted pole of (010) now lies very close to the true high-temperature curve close to the Linosa specimen (fig. 6*b*). The positions of the optic axes are likewise affected. Optic axis A moves only slightly, but optic axis B moves down the curve towards the centre of the stereogram

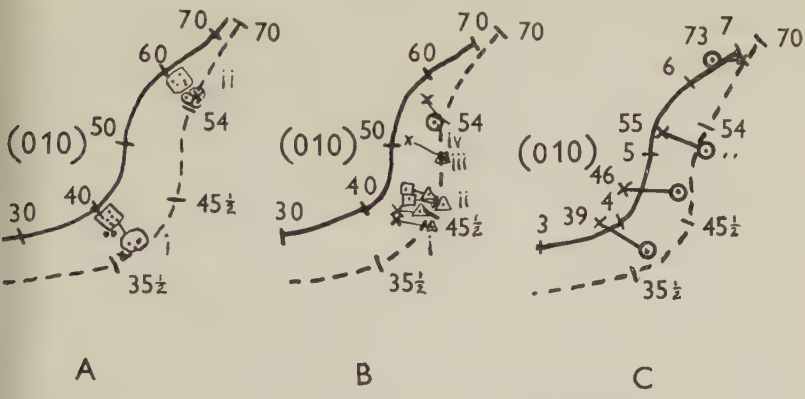

FIG. 6. Migration curves of the (010) pole for high- and low-temperature plagioclase showing the effect of heat-treatment on various felspars.

A (i) Esterel andesine for 404 hours at 1000° C. Original poles ⁘, after 404 hours ⊙ (C. T. Barber, 1936*b*). Plain dots, author's measurements on similar material. Position of pole after heating for 72 hours at 1000° C. is indicated by the cross.

(ii) Labradorite, St. John's Point, County Down. Original poles ⁘, after heating to 1000° C. for 404 hours ⁛ (data on heated material by C. T. Barber 1936*b*). Ringed dot, author's measurements on material heated to 1250° C. for 72 hours.

B (i) Andesine from Beaver Bay diabase. Original poles ×, after heating for 72 hours at 1000° C. as △.

(ii) Andesine from New Amalfi dolerite EH52. Original poles ⁛, after heating for 72 hours at 1000° C. △.

(iii) Labradorite from New Amalfi dolerite EH20. Original poles ×, after heating for 72 hours at 1000° C. △.

(iv) Labradorite from New Amalfi augite-hypersthene-dolerite. Original poles ×, after heating for 72 hours at 1000° C. ⊙.

C 39 Oligoclase An_{39} Tvedestrand. Original pole ×, after 9 hours at 1100° C. ⊙ (Scholler, 1941).

46 Labradorite An_{46} (locality not stated). Original pole ×, after 300 hours at 1100° C. ⊙ (T. F. W. Barth, Norsk Geol. Tidssk., 1931, vol. 12, pp. 57–72). [M.A. 5–218.]

55 Labradorite An_{55} Gorodische. Original pole ×, after 8 hours at 1100° C. ⊙ (Köhler, 1941; Scholler, 1941).

73 Bytownite An_{73} Crystal Bay, Minnesota. Original pole ×, after 9 hours at 1300° C. ⊙ (Scholler, 1941).

without any marked change in 2V. There has been, therefore, a slight rotation of the position of the optic axial plane which is well shown by the displacement of its pole β in fig. 7. It would seem, therefore, that this plagioclase was not in the ultimate high-temperature state.

TABLE II. Analyses of plagioclases.

	1.	A.	2.	3.	4.
SiO_2	57·59	56·78	61·50	57·05	56·18
Al_2O_3	25·84	26·96	23·50	26·42	27·14
Fe_2O_3	0·92	0·52	0·64	0·71	0·54
FeO	n.d.	0·22	n.d.	n.d.	n.d.
MgO	trace	—	0·04	0·02	0·04
CaO	8·45	8·77	7·71	9·55	10·55
Na_2O	6·39	6·13	5·77	5·60	5·10
K_2O	0·55	0·42	0·79	0·64	0·55
H_2O+	0·32	0·26	0·39	0·16	0·16
H_2O-	0·05	0·01	0·10	0·10	0·08
	100·11	100·07	100·44	100·25	100·34
Composition Wt. %					
Or	3·1	2·2	5·00	3·7	3·1
Ab	54·1	53·1	48·73	48·0	44·5
An	42·8	44·7	38·36	48·3	53·4
			Qz ... 8·22		
Sp. gr.	2·681	2·685	—	—	—
α	1·551	1·552	1·550–3	1·553	1·556
β	1·555	1·556	1·555–8	1·558	1·561
γ	1·559	1·560	1·558–61	1·564	1·566
An	44·1	45·5	44·1	50·4	55·1

1. Andesine from iron-rich diabase, M3174. Beaver Bay, Minnesota.
A. Andesine from Linosa, Mediterranean (Ernst and Nieland, 1934, table VI; Analyst, H. Nieland.
2. Andesine from iron-rich dolerite, EH52. New Amalfi, South Africa.
3. Labradorite from quartz-dolerite, EH20. New Amalfi, South Africa.
4. Labradorite from augite-hypersthene-dolerite. New Amalfi, South Africa.

Analyses 1, 2, 3, and 4 by I. D. Muir. All refractive indices $\pm 0{\cdot}001$.

(ii) *Andesine from Monte Rosso, Linosa, Mediterranean.*

Because of the comparable compositions of the Beaver Bay andesin and one of the analysed Linosa felspars $An_{45\cdot5}$, it was considered desi able that specimens of this Linosa felspar should be obtained for X-ra study. As all the German material used by Ernst and Nieland and b Köhler was destroyed during the war, the study of these felspars wa carried out on a number of small glass-clear crystal fragments kindl supplied by the Trustees of the British Museum. These crystals ar part of the material, loose crystal lapilli, collected from Monte Rosso i Linosa by Washington and described by Washington and Wright i 1910. Washington's analyses carried out in triplicate showed th felspars to be deficient in silica, and he considered that they were soli solutions between anorthite, albite, and carnegieite and named ther 'anemousite'. Later work by Ernst and Nieland, who described a

extensive collection of felspars from a similar locality in the same part of the island, established that they were chemically normal plagioclases with deviating optical properties.

The new determinations of the optical orientation, figs. 3*c* and 7, are in agreement with Ernst and Köhler's measurements and Wright's

FIG. 7. Showing the rotation of the pole of the optic axial plane (β) produced by heat-treatment of various felspars for 72 hours at 1000° C.

(i) Andesine from Beaver Bay diabase M3174. Original poles •, after heat-treatment ×.
(ii) Andesine EH52, New Amalfi. Original poles ⊙, after heat-treatment ⊕.
(iii) Labradorite from EH20, New Amalfi. Original poles •, after heat-treatment ⊗.
(iv) Labradorite from augite-hypersthene-dolerite, New Amalfi. Original poles •, after heat-treatment ⊕.
E. Esterel andesine. L. Poles of fragments of Linosa felspars.

extinction angles, and confirm both Ernst and Nieland's and Washington and Wright's observations that although each crystal is quite homogeneous chemically, different crystals vary considerably in composition. X-ray oscillation photographs about the *a*-, *b*-, and *c*-axes confirm that the minerals are in the high-temperature state, having a 7 Å. *c*-axis.

In view of Washington's analytical data on this plagioclase and the doubt about the localities of the two collections, one-tenth of a gram of plagioclase free from inclusions was separated on the isodynamic

separator. Because of the limited quantity of material available (fragments from crystals of different chemical compositions) it was not possible to undertake a further separation by means of heavy liquids to obtain a chemically homogeneous sample for analysis as both Washington and Nieland had done.

TABLE III. Analysis of plagioclase from Linosa, Mediterranean.

	I.	Mol. Prop.	Or.	Ab.	An.	Σ.		
SiO_2	54·44	0·907	0·021	0·540	0·374	0·935	Composition wt. %	
Al_2O_3	28·97	0·284	0·0035	0·090	0·187	0·2805	Or	1·94
Fe_2O_3	0·51	0·003	—	—	—	—	Ab	43·49
MgO	0·13	0·003	—	—	—	—	An	51·99
CaO	10·47	0·187	—	—	0·187	—	Ne	1·99
Na_2O	5·57	0·090	—	0·090	—	—		99·41
K_2O	0·35	0·0035	0·0035	—	—	—		
	100·44						Felspar to 100 %	
							Or	1·8
							Ab	46·7
							An	51·5
	A.							
SiO_2	52·77	0·8795	0·048	0·522	0·380	0·950	Composition wt. %	
Al_2O_3	29·50	0·289	0·008	0·087	0·190	0·285	Or	4·32
Fe_2O_3	0·65	0·009	—	—	—	—	Ab	37·52
FeO	0·17	—	—	—	—	—	An	52·32
MgO	0·05	—	—	—	—	—	Ne	5·24
CaO	10·66	0·190	—	—	0·190	—		99·40
Na_2O	5·40	0·087	—	0·087	—	—		
K_2O	0·74	0·008	0·008	—	—	—		
H_2O-	0·36	—	—	—	—	—	Felspar to 100 %	
	100·30						Or	4·3
							Ab	44·3
							An	51·4

I. Plagioclase from Monte Rosso, Linosa. Collected by H. S. Washington Analyst, J. H. Scoon.

A. Plagioclase ('anemousite') from same locality. Average of three duplicate analyses by H. S. Washington. (Washington and Wright, 1910.)

The analysis was carried out on a semi-micro scale by Mr. J. H Scoon, and the results are quoted in table III along with Washington's average of three analyses. From the recalculation of the analysis it is clear that it conforms well with the plagioclase structural formula, as do the analyses by Nieland.

Another analysed high-temperature plagioclase conforming with the curves determined for the Linosa minerals is that from the andesite (An_{38}) of Mayeamo, Japan, described by Becke (1921).

(iii) *Andesine An_{40}, NW. of Agay, Esterel, France.*

This famous andesine occurs as phenocrysts in an andesite and is associated with a deep-bluish amphibole. It is mentioned by Köhler (1941) but was not used for drawing up his curves because it deviated from them. Actually Köhler quotes the position of optic axis A incorrectly in his paper and the author's data agree with Becke's and Barber's measurements (fig. 6). On heat-treatment the pole of (010) which lies off the low-temperature curves moves on to the high temperature curve at about the appropriate composition and the optic axes also show a slight movement. These results too are in agreement with those obtained by Barber (1936*b*) on the same material. X-ray oscillation photographs on the unheated mineral confirm that it too has a 7 Å. *c*-axis. It must be concluded, however, that this mineral also is not truly in the ultimate high-temperature state.

(iv) *Andesine An_{45-48}, New Amalfi intrusive sheet, South Africa.*

Three plagioclases from this intrusion have been studied, one from the iron-rich facies of the dolerite being the most sodic. The rock from which the plagioclase was separated (EH52, Poldervaart, 1944) is rather similar in petrographic character to the Beaver Bay specimen. The ferroaugite is of similar composition to the Beaver Bay one but the exsolution lamellae parallel to (001) are more conspicuous. No separate pigeonite occurs and there is a little interstitial primary orthopyroxene (Of_{73}) and olivine (Fa_{85}).

The plagioclase has the same general textural features as the Beaver Bay andesine but is more markedly zoned towards the margins. Albite-Ala fourlings are again present and were used for determining the optical orientation. Unlike the Beaver Bay and Esterel andesines, this mineral exhibits very fine hair-like albite lamellae within the principal twin sub-individuals. Because of the more pronounced zoning of this felspar, the central portions of the crystals only were used for determining the optical orientation.

The results of the optical measurements made on this plagioclase are given in the composite stereograms, figs. 3*b*, 4, and 5, where it can be seen that both the (010) pole and of optic axis A (for ten crystals) lie in positions nearly half-way between the high- and low-temperature curves at compositions averaging about 46 % An. This composition is confirmed by the refractive index measurements made on a specimen near the centre of the field of scatter. A portion of this crystal was used for heat-treatment.

Oscillation photographs of the unheated material show only a fe very feeble subsidiary doubled type '*b*' reflections on the *c*-axis photo graphs. On heat-treatment for 72 hours at 1000° C. the poles of (010 and β move close to the high-temperature curves.

The optical and X-ray data both confirm that this plagioclase a is in a transitional state, but is in a rather different structural conditio to the Beaver Bay andesine because of a rather slower rate of cooling a conclusion which had already been inferred from the broader natur of the exsolution lamellae of the ferroaugite in the New Amalfi rock.

An analysis of the plagioclase fraction separated from this rock is giv in table II, column 2. In this case it is clear that the analysed mater contained about 10 % of quartz from the groundmass of the rock a also a proportion of the more sodic late plagioclase.

(v) *Labradorites from the New Amalfi intrusive sheet, South Africa.*

In order to obtain a clearer idea of any relation between the structu state of the plagioclase and exsolution and inversion of the associate pyroxenes, two felspars from earlier two-pyroxene rocks of this in trusion were examined and analysed.

The first of these (EH20, Poldervaart, 1944), from a rock which mus have crystallized from a liquid very close to the limit of the two-pyroxen field, contains ferroaugite $Ca_{35}Mg_{31}Fe_{34}$ (α 1·706, β 1·711, γ 1·73 2V 48–50°), with exsolution lamellae parallel to (001) which are perha a little coarser than those of the ferroaugite of EH52. The lime-poo pyroxene was a pigeonite and is now represented by orthopyroxe (β 1·731, 2V 53°) Of_{59} with fine but distinct exsolution lamellae of augi parallel to the original (001). The plagioclase (An_{51}) is generally simil to that of EH52, but is much less strongly zoned and contains relative few large untwinned areas. Around the margins of such areas as rema untwinned the hair-like subsidiary albite-twin lamellae pinch ou Twinning is chiefly on the albite, Carlsbad, and pericline laws. Optic measurements show that for this felspar the plotted poles of (010) again in an intermediate position between the high- and low-temperatu curves (fig. 3*a*).

The second plagioclase studied (An_{55}) came from a more basic rock the same intrusion. The associated pyroxenes are augite $Ca_{37}Mg_{53}Fe$ (α 1·674, β 1·680, γ 1·702, 2V 40–48°, average value 44°), and orth pyroxene Of_{39} (β 1·712, 2V 53°) with fine well-developed exsolutio lamellae of augite parallel to (100) and an outer zone containing abunda inclusions of the same mineral. The augite contains two sets of e

solution lamellae, a broad set parallel to (001) and a much finer set parallel to (100). On the evidence of the pyroxenes this rock would seem to have cooled much more slowly than the preceding one.

The plagioclase (An_{55}) is clear, unaltered, and devoid of zoning. It builds short subhedral crystals with broad (0·1 mm.) distinct twin lamellae, contains relatively few large untwinned areas, and has the usual fine hair-like albite twin lamellae. Twinning is chiefly on the albite, albite-Carlsbad, pericline, and Carlsbad laws, and one example of Manebach-acline twinning was observed. The plotted pole of (010) deviates only slightly from Reinhard's (low-temperature) curve but lies on the curves of Spaenhauer as given by Barber (1936*a*) and of van der Kaaden (1951). On heating to 1000° C. for 72 hours the poles of (010) of selected crystals of both of these specimens moved on to the high-temperature curve at the appropriate compositions (fig. 6*b*).

X ray oscillation photographs of both specimens show that the type *b*' reflections are doubled in the normal manner of the intermediate plagioclases: but a rough comparison of the relative intensities of the subsidiary reflections for a particular oscillation range suggests that those of the second specimen are slightly stronger than those of the first, and the character of the pattern for the second specimen is that of a normal low-temperature plagioclase. It is known (Gay, 1954) that the intensities of the subsidiary reflections fade on heating but the precise variation in the intensities of the subsidiary reflections with composition is not known. For the range An_{51-55} the intensity change (if any) will be very small, so it seems reasonable to suggest that the first specimen (EH20) with the slightly weaker reflections is not completely inverted but is not far from the true low-temperature state. A full account of the X-ray patterns of these and other felspars mentioned in this paper will be included in a later publication by Gay describing X-ray work on the intermediate plagioclases.

V. The relation between exsolution and inversion of the pyroxenes and the structural state of the plagioclase.

The study of the specimens described in the previous section shows clearly that there is a definite relation between exsolution and inversion in the pyroxenes whose compositions are plotted in fig. 8, and the structural condition of the associated plagioclase. Where iron-rich pigeonite remains, as in the rocks from the summit of Mount Wellington, Tasmania, the plagioclase (An_{55}) has remained in the high-temperature

state, as the plotted positions of the (010) poles demonstrate quite clearly (fig. 3*c*). In this rock very fine exsolution lamellae of pigeonite can also be observed in the ferroaugite. At Beaver Bay some of the pigeonite has inverted to orthopyroxene and the plagioclase (An_{44}) is in a transitional condition although it still retains its 7 Å. *c*-axis. The

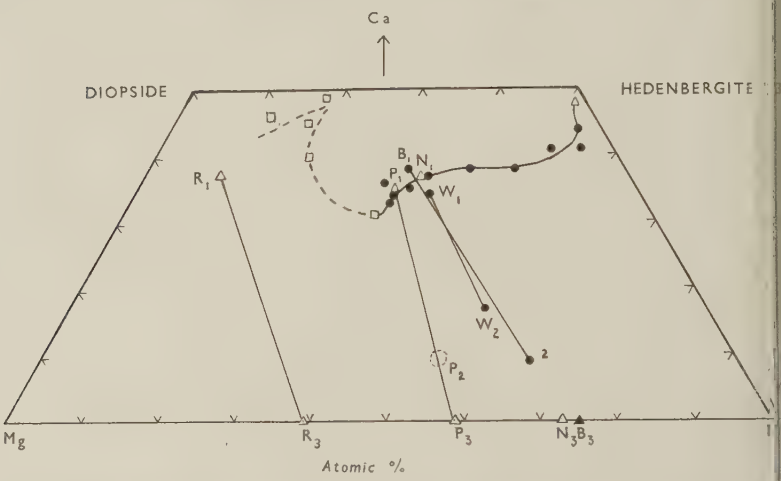

FIG. 8. Pyroxenes associated with felspars from tholeiitic rocks discussed in the paper. Comparison is made with the normal clinopyroxene trend of the Skaergaard intrusion (Muir, 1951). In this diagram the lime-content of the orthopyroxenes is ignored.

• Analysed pyroxenes. △ ▲ Composition estimated from optical properties. □ Clinopyroxene composition recalculated from analysis of bulk pyroxene of the rock.

B. Beaver Bay diabase M3174. B_1 ferroaugite, B_2 pigeonite, B_3 primary orthopyroxene.

N. New Amalfi iron-rich dolerite EH52. N_1 ferroaugite, N_3 primary orthopyroxene.

P. New Amalfi quartz-dolerite EH20. P_1 ferroaugite, P_3 inverted orthopyroxene. P_2 inferred composition of original pigeonite.

R. New Amalfi augite-hypersthene-dolerite. R_1 augite, R_3 primary orthopyroxene.

W. Mount Wellington sill, Tasmania. Dolerite of summit. W_1 ferroaugite, W_2 pigeonite. (Analyses to be published in a later paper.)

next stage is represented by the minerals of the rock EH52. Here exsolution lamellae in the ferroaugite are better developed and the plagioclase (An_{46}) now shows feeble subsidiary reflections. A still slower rate of cooling is represented by the rock EH20 where the pigeonite has just inverted and the plagioclase (An_{51}) is still not completely in the

low-temperature state. In this rock the exsolution lamellae of the ferroaugite still retain their oblique extinction and high birefringence, and appear to be pigeonite. No rock containing the necessary iron-rich pyroxenes could be found to serve as an example of the final stage, which is represented instead by the minerals of the last specimen described where the pyroxenes are rich in magnesia. In this rock the augite contains very broad exsolution lamellae parallel to (001) composed of orthopyroxene the exsolved material itself having inverted from pigeonite. The plagioclase of this rock is in the normal low-temperature state.

VI. The development of secondary twinning in plagioclase.

A significant feature of several of the crystals subjected to heat-treatment was the development of new albite and pericline twinning. Possibly the best illustration of this was afforded by the heat-treatment of a primary albite-twin crystal of the Beaver Bay andesine (fig. 9*a*). Before heating, this crystal contained only a few very fine hair-like subsidiary albite twin lamellae (arrowed in figure) and no lamellae of pericline type. After heating, the subsidiary albite lamellae had become much more numerous and a few of pericline type had also appeared. A similar development of new twinning by heating has been reported by Scholler (1941) in the bytownite (An_{73}) from Crystal Bay, Minnesota. It has been observed also by the author in heat-treated specimens of labradorite (An_{62}) from St. John's Point, Co. Down, on which X-ray data have been provided by Gay and Taylor (1953), and an anorthite An_{98} from Pasmeda Alp, Fassa. The production of fine albite and pericline twinning is also recorded by Tuttle and Bowen (1950) in heat-treated Amelia albite. The twinning in this case can probably be attributed solely to the low–high temperature inversion, for the differences between low- and high-temperature albite are of considerably greater magnitude than those existing between comparable low- and high-temperature forms in the more basic plagioclases.

No obvious explanation of this new twinning can be offered, at this stage, on the above evidence alone, but it is of interest to note that all three intermediate plagioclases in which it was developed are transitional types close to the high-temperature structural state and contain large untwinned areas.

In order to investigate further the significance of this fine twinning, two plagioclase crystals from the specimen EH20 where the mineral is close to the low-temperature state were selected for heat-treatment

and cut out of a thin section. These crystals showed what was regard... as a partial development of secondary twinning (fig. 9*b*), and contain... relatively large untwinned areas. These are uncommon in this plag... clase. Unfortunately, the crystals broke up on being removed from t... crucible after heat-treatment at 1000° C. for 72 hours, but examinati...

FIG. 9*a*. Albite-twinned plagioclase crystal from Beaver Bay diabase, showin... newly developed albite and pericline twin lamellae after heat-treatment for 4... hours at 1000° C. Original lamellae indicated by arrows. ×50.

of the heated material revealed numerous fine albite-twin lamellae an... no large untwinned fragments. Similar fine lamellae may be observe... in many low-temperature plagioclases which are thought to have passe... through the high-temperature state.

The twinning of another crystal (fig. 9*c*) from this specimen is o... interest. This crystal is one of the rare examples in the rock where ... large primary albite-twin sub-individual is almost devoid of subsidiar... lamellae. The other sub-individual, however, has well-developed lamella... of albite and pericline type. Both halves of the crystal are zoned to ... similar degree at the margins to An_{42}, but the central portions of th... crystal are quite homogeneous and have the same composition (An_{51})... Although repeated measurements on the universal stage gave consisten... results in all four major sub-individuals it was impossible to locate th... albite twin axis accurately on the projection because of the large triangl... of error formed by the intersections of the great circles. The reason fo...

This became obvious when the poles of (010) for the two major sub-individuals were plotted on a stereogram using the cleavage and composition plane as reference directions (fig. 10). From this it can be seen that there is no difference in composition between the two sub-

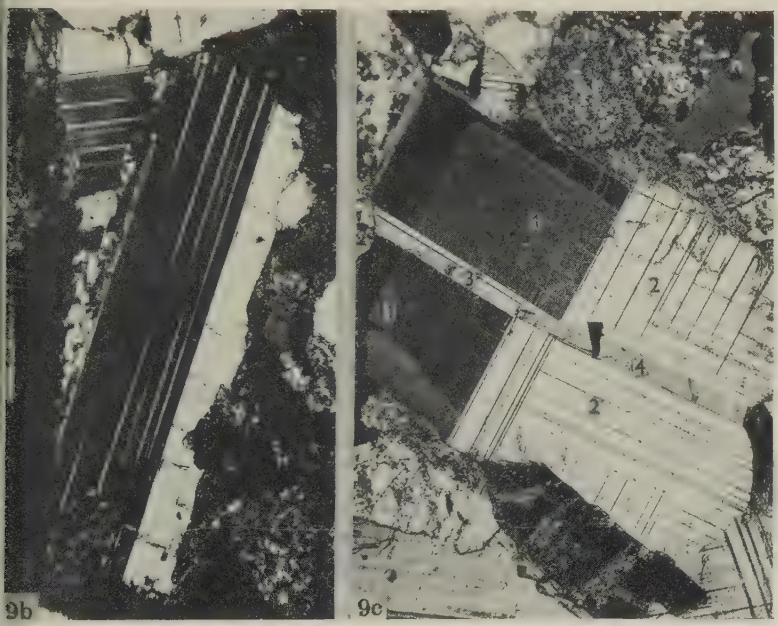

Fig. 9*b*. Andesine crystal from quartz-dolerite EH20, New Amalfi, South Africa, showing a partial development of subsidiary albite-twin lamellae around the margins of the crystal. ×24.

Fig. 9*c*. Primary albite-twinned plagioclase from quartz-dolerite EH20, New Amalfi.

Sub-individuals 1 and 2 albite twinned; 1 and 3, and 2 and 4 pericline twinned. Note the development of fine subsidiary twin lamellae in the right-hand side of the crystal only. ×24.

individuals, but it seems likely that the inversion has proceeded farther in that portion of the crystal in which the subsidiary twin lamellae are abundant. The difference in the mean positions of the plotted poles ($3\frac{1}{2}°$) is significant, but must be regarded as being just within the limits of experimental error in view of the fact that the (010) composition plane and cleavage, and not the twin axis, must be used as a reference direction in cases such as this. It is hoped that it will be possible to carry out

further work on similar crystals supported by X-ray work to try and confirm the conclusions suggested here by the optical data.

The evidence thus far would seem to indicate that the development of this secondary twinning was in some way dependent on the rate of cooling. It might be thought that this twinning would be induced by the strain caused by the inversion from the high- towards the low-temperature state; but if this was the case then it is difficult to understand, firstly, why new lamellae are produced by heating the mineral

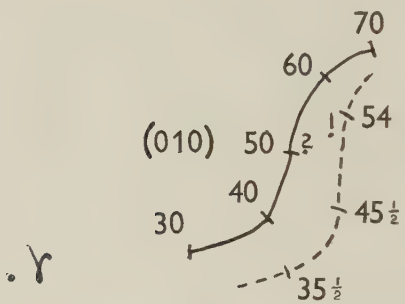

FIG. 10. Migration curves for high- and low-temperature plagioclases, showing the positions of the (010) face pole for the two major sub-individuals of the crystal illustrated in fig. 9*c*.

when they should disappear, and secondly, why intermediate plagioclases can exist apparently quite stably in various transitional states in considerable structural strain is induced by the inversion. Rather does it seem that the secondary twinning was incipient in the original high-temperature plagioclase and developed during slow cooling as a separate feature which may be independent of the inversion. In this case subsequent annealing to 1000° C. could allow more of these fine lamellae to develop.

Careful detailed studies of plagioclase twinning have shown that much of the twinning seems to be primary. The fine lamellae present in many intermediate plagioclases seem to be of secondary origin. It may well be that many of the coarser polysynthetic lamellae of natural igneous plagioclases have a similar origin, for many of them seem to have developed late in the history of the crystal. Only a long and detailed study of high-temperature, transitional, and low-temperature plagioclases of similar compositions and parageneses will be able to shed further light on this problem, the solution of which might have great petrogenetic significance.

Acknowledgements. The author wishes to thank Professor C. E. Tilley and Dr. W. H. Taylor for constant help and interest in the progress of this work and for criticism of the manuscript. To my colleague Dr. P. Gay also many thanks are due for numerous helpful discussions on plagioclase problems and for interpretation of the X-ray photographs. The Trustees of the British Museum very generously supplied fragments of Washington's Linosa 'anemousite' on which Mr. J. H. Scoon kindly carried out a semi-micro analysis. The X-ray photographs were taken by Mr. K. Rickson.

References.

Barber (C. T.), 1936*a*. The Tertiary igneous rocks of the Pakokku district and the Salingyi township of the Lower Chindwin district, Burma, with special reference to the determination of the felspars by the Fedoroff method. Mem. Geol. Surv. India, vol. 68, pp. 121–292. [M.A. **7**–21.]

——, 1936*b*. The effects of heat on the optical orientation of plagioclase felspars. Min. Mag., vol. 24, pp. 343–352.

Becke (F.), 1921. Die optischen Eigenschaften einiger Andesine. Tschermaks Min. Petr. Mitt., vol. 35, pp. 31–46. [M.A. **2**–61.]

Buerger (M. J.), 1948. The rôle of temperature in mineralogy. Amer. Min., vol. 33, pp. 101–121. [M.A. **10**–380.]

Chayes (F.), 1952. Relations between composition and indices of refraction in natural plagioclase. Amer. Journ. Sci., Bowen vol., pp. 85–105. [M.A. **12**–134.]

Chudoba (K.) and Engels (A.), 1937. Der Einfluß der Kalifeldspatkomponente auf die Optik der Plagioclase. Zbl. Min. Abt. A., 103–116. [M.A. **7**–21.]

Cole (W. F.), Sörum (H.), and Taylor (W. H.), 1951. The structures of the plagioclase felspars. I. Acta Cryst., vol. 4, pp. 20–29. [M.A. **11**–427.]

Ernst (E.) and Nieland (H.), 1934. Plagioklase von Linosa, ein Beitrag zur Anemousitfrage. Tschermaks Min. Petr. Mitt., vol. 46, pp. 93–126. [M.A. **6**–118.]

Gay (P.), 1953. The structures of the plagioclase felspars: III. An X-ray study of anorthites and bytownites. Min. Mag., vol. 30, pp. 169–177.

——, 1954. The structures of the plagioclase felspars. V. The heat-treatment of lime-rich plagioclases. Min. Mag., vol. 30, pp. 428–438.

—— and Taylor (W. H.), 1953. The structures of the plagioclase felspars. IV. Variations in the anorthite structures. Acta Cryst., vol. 6, pp. 647–650. [M.A. **12**–333.]

Grout (F. F.) and Schwartz (G. M.), 1939. The geology of the anorthosites of the Minnesota coast of Lake Superior. Bull. Minnesota Geol. Surv., no. 28. [M.A. **8**–242.]

Kaaden (G. van der), 1951. Optical studies on natural plagioclase feldspars with high- and low-temperature optics. Diss. Univ. Utrecht. [M.A. **11**–282.]

Köhler (A.), 1941. Die Abhängigheit der Plagioklasoptik vom vorangegangenen Wärmeverhalten. Tschermaks Min. Petr. Mitt., vol. 53, pp. 24–49. [M.A. **8**–313.]

Laves (F.), 1952. Phase relations in the alkali feldspars. Journ. Geol., vol. 60, pp. 436–450 and pp. 549–574. [M.A. **12**–136.]

Muir (I. D.), 1951. The clinopyroxenes of the Skaergaard intrusion, eastern Green-land. Min. Mag., vol. 29, pp. 690–714.

——, 1954. Crystallization of pyroxenes in an iron-rich diabase from Minnesota. Min. Mag., vol. 30, pp. 376–388.

Oftedahl (C.), 1948. Studies on the igneous rock complex of the Oslo region. IX. The feldspars. Skrifter Norske Viden. Akad., Oslo, Math.-Nat. Kl., no. 3, pp. 1–71. [M.A. **11**–11.]

Poldervaart (A.), 1944. The petrology of the Elephants' Head dike and the New Amalfi sheet (Matatiele). Trans. Roy. Soc. South Africa, vol. 30, pp. 85–119.

Reinhard (M.), 1931. Universal Drehtischmethoden. Basel. [M.A. **4**–435.]

Scholler (H.), 1941. Versuche zur Temperaturabhängigkeit der Plagioklasoptik. Tschermaks Min. Petr. Mitt., vol. 53, pp. 180–221. [M.A. **8**–313.]

Tertsch (H.), 1942. Zur Hochtemperaturoptik basischer Plagioklase. Tschermaks Min. Petr. Mitt., vol. 54, pp. 193–217. [M.A. **9**–270.]

Tuttle (O. E.) and Bowen (N. L.), 1950. High-temperature albite and contiguous feldspars. Journ. Geol., vol. 58, pp. 572–583. [M.A. **11**–327.]

—— and Keith (M. L.), 1954. The granite problem: evidence from the quartz and feldspar of a Tertiary granite. Geol. Mag., vol. 91, pp. 61–72. [M.A. **12**–418.]

Wager (L. R.) and Deer (W. A.), 1939. Geological investigations in east Greenland. Part III. The petrology of the Skaergaard intrusion, Kangerdlugssuaq, east Greenland. Medd. om Gronland, vol. 106, no. 4, pp. 1–352. [M.A. **8**–27.]

Washington (H. S.) and Wright (F. E.), 1910. A feldspar from Linosa and the existence of soda anorthite (carnegieite). Amer. Journ. Sci., Ser. 4, vol. 29, pp. 51–70.

An accurate determination of the cell dimensions of bultfonteinite, $Ca_4Si_2O_{10}H_6F_2$.

By Helen D. Megaw, M.A., Ph.D., F.Inst.P., and C. H. Kelsey, B.A.

Crystallographic Laboratory, Cavendish Laboratory,
University of Cambridge.

[Read January 27, 1955.]

BULTFONTEINITE from Bultfontein mine, Kimberley, South Africa, is a hydrated fluorine-containing calcium silicate, of approximate composition $Ca_4Si_2O_{10}H_6F_2$. It was first described in 1932 by Parry, Williams, and Wright,[1] who gave an account of its morphology, optical properties, composition, and chemical relationships. It is triclinic but markedly pseudo-orthorhombic. The present work consists primarily of a determination of the unit-cell dimensions, involving a more accurate evaluation of the interaxial angles than the earlier one; this is followed by some tentative suggestions about the structure.

The material examined was kindly provided by the late Mr. A. F. Williams. Most of the crystals could be seen optically to be very much twinned, but it was possible to pick out small lath-shaped fragments, a few tenths of a millimetre in length, which showed uniform extinction over most of their area. X-ray observations were made on three fragments of this kind; crystal 3 had a uniform interference colour over its whole area, crystal 1 had a small stripe of a different colour near the edge, and crystal 2 was slightly wedge-shaped.

The approximation to orthorhombic symmetry made it easy to set the crystal. Oscillation photographs (with Cu-$K\alpha$ radiation) taken about two axes gave rough values of all three cell edges, which enabled all reflections to be indexed. The face of largest area was parallel to (100). Twinning was present in all three crystals, but it proved possible to interpret it and to establish the twin laws.

Twinning.

With the first crystal, oscillation photographs about the needle axis z gave reflections on layer lines only, showing that all twin components

[1] J. Parry, A. F. Williams, and F. E. Wright, Min. Mag., 1932, vol. 23, p. 145.

had strictly parallel z-axes. In oscillation photograph about y, however, strong spots on the layer lines had weaker companions off the layer line but on the same row line, and also companions of about half their own intensity on the same layer line; these latter, if not too weak, had themselves row-line companions. This showed the presence of twinning about the normals to (100) and (010), the former giving rise to components more nearly equal in volume than the latter. However, there was no detectable vertical splitting of reflections $h00$, even for $h = 14$. This could only be true if the angle (100):(010) were very close to 90°; the splitting should have been observed if the difference was greater than 10′.

Crystal 2 showed the same kind of twinning; crystal 3 (optically the most uniform) showed twinning about the normal to (100) only. These results fit in with the optical observations if the composition plane is normal to the twin axis, since twinning about the normal to (100) would still lead to a uniform appearance of the crystal viewed through this face.

It is worth drawing attention at this point to the interaxial angles listed in table I. Since α^* differs from 90° more than does β^*, the difference of angle between the z^*-axes of the two components will be greater in a twin about the normal to (010) than in one about the normal to (100). Thus the twin law which is observed experimentally to be more prevalent is the one which involves the smaller geometrical misfit.

Accurate determination of spacings.

An ordinary Unicam cylindrical camera was used. The setting of the crystal with respect to the circle was found from ordinary oscillation photographs. Then a film was inserted in the van Arkel position, and the crystal was given appropriate oscillations so that selected high-angle reflections were recorded on the film on either side of the beam. The distance between the spots was measured on a simple comparator with vernier reading to $\frac{1}{10}$ mm.

The method used here may be compared with those of Farquhar and Lipson[1] and Weisz, Cochran, and Cole.[2] Essentially it combines the photographic technique of the former (in a simplified form which involves no special modifications to the camera) with the treatment of the data used by the latter in their 'θ-method'. Like the 'θ-method', it relies entirely on measurement of a few high-angle reflections, and its

[1] M. C. M. Farquhar and H. Lipson, Proc. Physical Soc., 1945, vol. 58, p. 200.

[2] O. Weisz, W. Cochran, and W. F. Cole, Acta Cryst., 1948, vol. 1, p. 83. [M.A. 10–330.]

accuracy is about the same. It does not aim at the very high accuracy which can be attained in favourable cases, at the expense of much more labour, by graphical extrapolation from a large number of reflections.

Calculation and choice of reflections.

(i) *Oscillation about y-axis.*—For any reflection in the [010] zone, we have

$$\xi^2(h0l) = h^2a^{*2}+l^2c^{*2}+2hla^*c^*\cos\beta^* \qquad (1)$$

where a^*, c^*, β^* are axial lengths and interaxial angle of the reciprocal lattice, and $\xi = 2\sin\theta$. Since ξ is directly determinable from the photographs, it is possible by measurement of a number of $h0l$ spacings to determine a^*, c^*, and β^* from equation (1). The choice of reflections to be used is determined primarily by the requirement that θ shall be nearly 90°, since this is necessary for accuracy; convenience of mathematical handling of the equations takes second place. For a crystal in which β^* is nearly 90°, it is an obvious choice to use pairs of reflections $h0l$, $h0\bar{l}$, since they occur at nearly the same value of θ. If the crystal is twinned about the normal to (100), they have the further advantage of appearing within the same oscillation range, so that one exposure serves to record both. Then

$$\xi^2(h0\bar{l}) = h^2a^{*2}+l^2c^{*2}-2hla^*c^*\cos\beta^*,$$

hence

$$\tfrac{1}{2}[\xi^2(h0l)+\xi^2(h0\bar{l})] = h^2a^{*2}+l^2c^{*2} \qquad (2)$$

$$\tfrac{1}{2}[\xi^2(h0l)-\xi^2(h0\bar{l})] = 2hla^*c^*\cos\beta^*. \qquad (3)$$

Thus $\cos\beta^*$ can be determined easily with high accuracy.

For bultfonteinite, 14,0,0 gave a reflection at about 80°, enabling a^* to be determined immediately. The pair of reflections 307, $30\bar{7}$ then could be used to evaluate c^* and β^*. Other reflections available were 207, $20\bar{7}$; 12,0,2, 12,0,$\bar{2}$. Comparison of the c^* values derived from these reflections of different θ (all greater than 60°), and from photographs with and without black paper between film and camera, enabled a check to be made of the effective camera radius (i.e. the radius of the shrunk film after development). It proved to be exactly 3 cm. when the black paper was used. If the paper was omitted, the relative error in the spacing amounted to only 2×10^{-4} for a reflection at $\theta = 80°$. Film shrinkage of 0·3 %, if not allowed for, would give an error of the same magnitude; variations of shrinkage from one film to another are likely to be much less than this. This emphasizes the usefulness, when accuracy is required, of concentrating on high-angle reflections.

Values of β^* were derived from the three pairs of planes mentioned above, using the known a^* and c^*, and the mean value was taken.

(ii) *Oscillation about z-axis.*—A crystal mounted to rotate about the z-axis was used to obtain b^* and γ^*, the former from 4,10,0, the latter from the pair 790, $7\bar{9}0$, by the method of successive approximations. In this, a rough value of b^* was used to find γ^* from 790, $7\bar{9}0$; this was then substituted in the expression for calculating b^* from 4,10,0, and the new value of b^* in its turn used to get an improved value of γ^*. This method leads in the end to better values for both quantities than the use of a single pair of reflections, since 4,10,0 is more sensitive to changes in b^*, than 790 and $7\bar{9}0$ to changes in γ^*: and it saves the extra work of measuring the spacing of $4,\bar{1}\bar{0},0$.

(iii) *Oscillation about x-axis.*—Finally, a crystal mounted about the x-axis was used to find α^* from the pair of reflections 056 and $05\bar{6}$ by the method of successive approximation. This pair had a lower value of θ than the reflections used in the other zones, and the results are correspondingly less accurate.

Results.

These are given in table I, with the morphological values for comparison. Several points should be noticed.

TABLE I. Lattice parameters of bultfonteinite.

	Present work.	Results of Parry, Williams, and Wright, 1932.
a	10·992±0·004 Å.	—
b	8·183±0·002	—
c	5·671±0·001	—
$a:b:c$ ...	1·3433:1:0·6930	½(1·3512):1:0·6873
α	93° 57′	94° 17′
β	91 19	91 59
γ	89 51	90 44
α^*	86° 03′±18′	85° 41′
β^*	88 41 ±02	87 57
γ^*	90 04 ±01	89 07

(1) The true unit cell is double the morphological cell in the a direction. Thus, to transform the indices of Parry, Williams, and Wright to the new indices, all values of h must be doubled.

(2) The angles determined in the present work differ very considerably from the old values. The old values are likely to be less accurate, because of the difficulty of goniometric measurements referred to by Parry, Williams, and Wright; their limits of error are in fact not stated.

In the present method, the pseudo-orthorhombic symmetry made conditions especially favourable to the attainment of high accuracy.

(3) The sense of the axes cannot be chosen so as to make all interaxial angles greater than 90°. The choice actually made seems in best agreement with the older work.

Structural relationships.

The formula of bultfonteinite may be written

$$Ca_3[SiO_3(OH)]_2.2H_2O.CaF_2,$$

in comparison with the structural formula of afwillite[1]

$$Ca_3[SiO_3(OH)]_2.2H_2O.$$

Parry, Williams, and Wright draw attention to this relationship in composition, and give arguments from chemical evidence suggesting that it is significant. Evidence from the cell dimensions points in the same direction. The *c*-spacing of bultfonteinite, 5·67 Å., is very nearly the same as the *b*-spacing of afwillite,[1] 5·63 Å., and in both cases this is morphologically the fibre axis. In afwillite one can pick out units of composition $Ca_2Si_2O_8$ consisting of Si tetrahedra and Ca octahedra linked together by shared edges in the direction of the fibre axis, and forming infinite pillars in this direction. They are the units into which an afwillite crystal would be subdivided by operation of the two prominent cleavage planes. In afwillite they are linked laterally by the third Ca atom into sheets, which in turn are held together only by hydrogen bonds and a few weak Ca–O bonds. It seems quite possible that a rearrangement of these pillars gives rise to the bultfonteinite structure, the two remaining Ca ions being available to link them together sideways, as well as the fluorine atoms which may form O–H–F bonds. It cannot be taken for granted that the H_2O groups persist as such; there may be complete rearrangement of the hydrogen atoms.

It is hoped that further work on this structure may be possible.

Acknowledgements.—The authors are very grateful to the late Mr. A. F. Williams for drawing their attention to this mineral as well as for supplying the crystals. One of us (C. H. K.) wishes to thank Girton College, Cambridge, for the award of a Studentship, and the Cement and Concrete Association for a grant while the work was being done.

[1] H. D. Megaw, Acta Cryst., 1952, vol. 5, p. 477. [M.A. **12**–98.]

The thermal reactions of nacrite and the formation of metakaolin, γ-alumina, and mullite.[1]

By G. W. Brindley, Ph.D., F.Inst.P.

College of Mineral Industries, Pennsylvania State University,

and K. Hunter, B.Sc.

Physics Department, University of Leeds.

[Taken as read January 27, 1955.]

1. Introduction.

FOR many years, a number of problems have persisted concerning the reactions which occur and the products which form when kaolinite and kaolin clays are heated to progressively higher temperatures. Between approximately 550° and 900° C., X-ray powder diagrams of kaolinite show mainly a broad band indicating either an amorphous, or a highly disordered, or a very finely dispersed state. The product is generally called metakaolin. At temperatures above 950° C. γ-alumina and mullite are formed. In some cases they appear together: in others the appearance of mullite is delayed. The relations of these products to each other and to the original kaolinite have received various interpretations and the course of the reaction is still disputed. Following an examination of nacrite from Hirvivaara, Finland (von Knorring, Brindley, and Hunter, 1952), we considered that a single crystal study of its thermal reactions might throw further light on those of kaolinite. The two minerals have a similar lamellar morphology and are composed of silicate layers having the same structure and the same chemical composition: they differ only in the stacking arrangements of the layers and in crystal size. The dehydration of nacrite follows a similar course to that of kaolinite and the ultimate products of decomposition are the same for the two minerals. It seems reasonable to suppose that their thermal reactions will be closely similar, though the particular temperatures at which reactions proceed may depend on crystal size.

[1] The experimental work described in this paper was carried out in the Physics Department, University of Leeds, in the period 1951–53. The paper was written and the data partly evaluated in the Mineral Science Building, Pennsylvania State University, Pa., U.S.A.

2. Experimental procedure.

Flakes of nacrite, about 0·2 0·5 mm. in size, were selected which, under the microscope and from X-ray rotation diagrams (fig. 1*a*), appeared to be of good crystalline quality. The best crystals showed a mosaic texture of the kind previously described for brucite (Brindley and Ogilvie, 1952) and which appears to be common for layer silicates. The *a*- and *b*-axes of a flake were determined prior to heat-treatment and subsequently they could be recognized by reference to irregularities in the outline of the flake. For X-ray study the crystals were mounted with shellac on fine glass fibres. For heat-treatment they were removed by alcohol from the shellac-coated fibres and placed in a platinum container. One flake was given as many as 20 heat-treatments between 500° and 1200° C. at about 50° intervals, each lasting 2–3 hours. The temperature was raised at the rate of about 15° C./min. and after treatment the crystals were cooled slowly in the furnace. Other flakes were heated directly to a particular temperature.

3. Results.

(*a*) *The metakaolin range, approximately 650–900° C.*

Rotation diagrams about the *b*-axis (*b* 5·15 Å. for nacrite) showed no more than a slight weakening of the reflections up to about 650° C., but at 670° C. a marked change occurred. The majority of the reflections then disappeared; those remaining (fig. 1*b*) formed a hexagonal pattern which, in terms of the *a*- and *b*-axes of nacrite, are indexed as 200, 110, 310. A rotation diagram about the normal to the flake, approximately *c*, showed streaks parallel to the rotation axis which could be indexed as 20*l*, 11*l*. No evidence was obtained for regularity normal to the flake surface. As the temperature was progressively raised, the hexagonal pattern of spots became weaker and a diffuse halo increased in intensity. The spot pattern was clearly visible up to 880° C. (fig. 1*c*).

The interpretation placed on these results is that, following the expulsion of the (OH) radicals from the structure, the layers retain a relict structure of hexagonal type having no detectable regularity from one layer to another. Since the (OH) radicals are expelled from the octahedral aluminium layer, it seems likely that the residual structural regularity is maintained by the Si–O hexagonal network. The relation of the Al atoms to this network, which has not yet been established, is

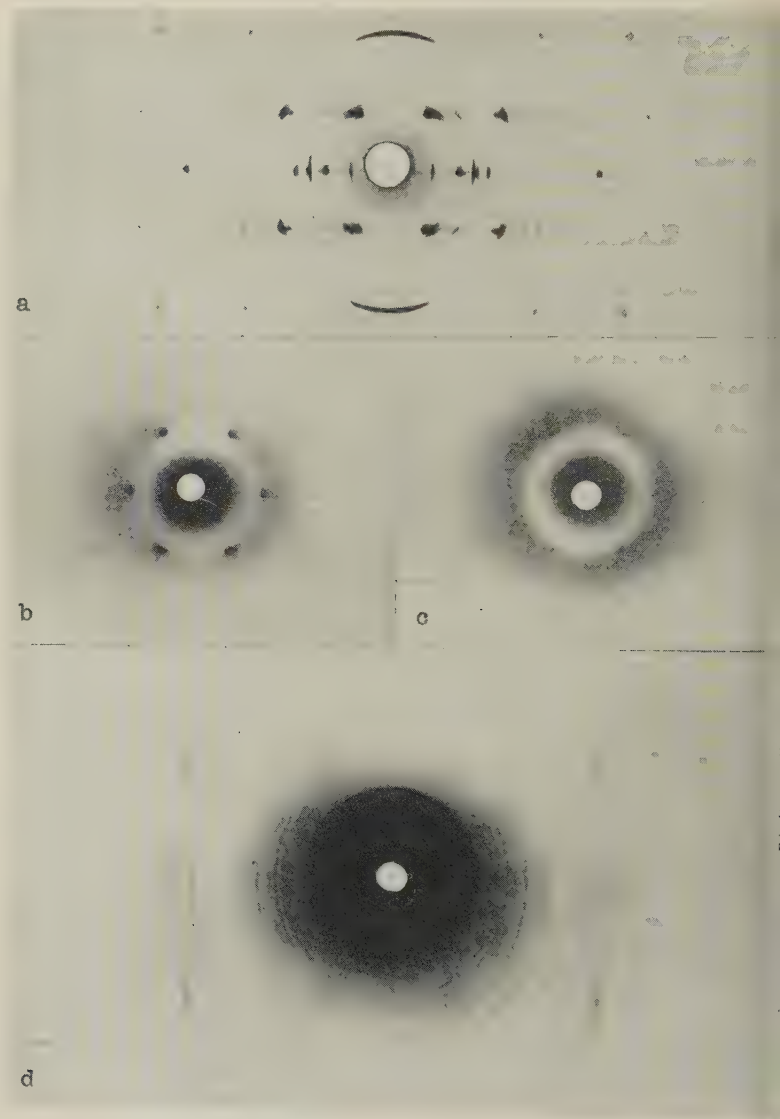

FIG. 1. (*a*) *b*-axis rotation diagram of nacrite. (*b*) *b*-axis diagram of the *same* nacrite crystal after heating to 670° C. (*c*) *b*-axis diagram of the *same* nacrite crystal after heating to 880° C. (*d*) *a*-axis rotation diagram of the *same* nacrite crystal after heating to 950° C.

discussed later. The results show clearly the persistence of a partially ordered phase up to about 900° C. which may be appropriately called metakaolin.

(*b*) *Formation of γ-alumina and mullite in the range 950–1150° C.*

No one disputes that mullite is the main product which ultimately forms on firing kaolinite to temperatures well above 1000° C. and the same is true for nacrite. The role of γ-alumina which forms at about 950° C. but disappears at higher temperatures and the true character of the exothermic reaction at about 950° C. have been much disputed.

The present work shows that when a single crystal flake is heat-treated at 950° C., the subsequent X-ray rotation diagram (fig. 1*d*, a rotation diagram about the *a*-axis of nacrite) contains a clear powder diagram in which a few lines show marked increases of intensity in particular directions indicating preferential orientation. The majority of the lines have a smooth distribution of intensity and can be attributed unambiguously to mullite; they correspond to a random distribution of small crystals. The lines showing orientation effects correspond to γ-alumina. This is a cubic, spinel-type structure giving relatively few strong lines. The following can be clearly recognized: 400 (I, 10; *d* 1·978); 440 (I, 10; *d* 1·387); 311 (I, 8; *d* 2·40); and 220 (I, 2; *d* 2·79), where I is the relative intensity given by Rooksby (1951) and *d* is the measured spacing. The variability of γ-alumina has been commented on by Bradley and Grim (1951) and interpreted in some detail by Ervin (1952); in the present work it has not been possible to study the γ-alumina in detail owing to the numerical preponderance of mullite lines in the X-ray diagram.

The evidence is conclusive that in these experiments γ-alumina forms with preferential orientation relative to the nacrite and the mullite has random orientation. This situation persists to 1150° C.

The presence of finely divided cristobalite is shown by a diffuse line at about 4·1 Å. corresponding to the strongest cristobalite reflection.

(*c*) *The second recrystallization at about 1150° C.*

The X-ray diagram clarifies considerably when the flake is heated to about 1150° C. The lines associated with γ-alumina which show marked orientation effects disappear at this temperature, the mullite pattern becomes clearer and more lines are visible. The pattern is still that of a random powder. It seems that the γ-alumina combines with cristobalite to produce more mullite. The greater clarity of the X-ray diagram

suggests not only *more* mullite, but a *better crystalline* product. Per sistence of the 4·1 Å. line indicates that excess silica remains as cristo balite.

(*d*) *Orientation of γ-alumina.*

The enhanced line intensities due to orientation (fig. 1*d*) have th appearance of a blurred rotation diagram with zero, first-, and secon order layer lines. The corresponding axis periodicities, which can be determined only very approximately, are 5·4 Å. from the first-orde and $2 \times 2{\cdot}78 = 5{\cdot}56$ Å. from the second-order layers. Taking the cubic cell parameter of γ-alumina as 7·88 Å. (Rooksby, 1951), we find the repeat distances [100] 7·88, [110] 11·14, and [111] 13·64 Å. The observed value admits of only one simple interpretation, viz. [220]. If [110] is the orientation axis, we expect to find only the even-order layers corresponding to $(h+k) = 0, 2, 4$, since γ-alumina is based on a face-centred lattice. This explains why we find the even-order repeat distances and not the odd-orders.

The details of the orientation diagram are fully consistent with this interpretation. The four reflections which are clearly recognized have the indices {220}, {311}, {400}, and {440}. The zero-order layer, with $h + k = 0$, shows $(2\bar{2}0)$, $(1\bar{1}3)$, (004), and $(4\bar{4}0)$. The first observed layer with $h + k = 2$, shows only (202) and (113) or $(3\bar{1}1)$, and no reflections of type {400} and {440}. The second observed layer, with $h+k = 4$, shows (220), (131), (400), and (404).

The clearest orientation diagram was obtained by rotation about the *a*-axis of a flake of nacrite heated directly to 950° C. Rotation about showed an appreciable enhancement of only the 440 reflection and on the equatorial level only. It appears that there is essentially a single orientation axis and that a fibre texture develops with [110] of γ-alumina parallel to *a* of nacrite.

4. Discussion of the present results in relation to the general problem of the thermal behaviour of kaolin clays.

(*a*) *Metakaolin.*

The present work shows clearly the persistence of some degree of crystalline order in the metakaolin phase. Its precise character is not established and the available diffraction data are wholly insufficient for a detailed analysis. It must be of hexagonal type and most probably takes the form of more or less flat Si–O hexagonal networks with little or no regularity between neighbouring networks. Previous workers

have come to somewhat similar conclusions and have advanced hypotheses regarding the relation between the Si–O network and the dehydrated alumina sheet of the kaolin structure.

In the earlier investigations, summarized by Richardson (1951), the diffraction band was considered to indicate an amorphous or nearly amorphous solid. More recent investigators have recognized that metakaolin is at least partially ordered. Tscheischwili, Büssem, and Weyl (1939), using crystal-reflected X-rays and a vacuum camera, observed the persistence of $hk0$ reflections from kaolinite far beyond the temperature at which dehydration occurs; these observations are in complete agreement with the present results for nacrite. They considered the diffraction band was very similar to that from silica-glass and concluded that the disordered part of the structure had a similar short-range order with both Si and Al ions tetrahedrally co-ordinated. They also suggested a model for the ordered metakaolin structure having the same Si–O tetrahedral layer as in kaolinite co-ordinated with an Al O tetrahedral layer; the latter tetrahedra are, however, very distorted and the Al–O distance, about 1·85 Å., is considerably greater than that generally found.

In a very detailed investigation, hitherto largely unknown due to wartime conditions, Eitel and Kedesdy (1944) (see also Eitel, 1954, pp. 1116–8) followed the thermal transformations of kaolinite by electron microscopy and electron diffraction. They showed the persistence of crystalline form up to high temperatures and observed the diffraction lines from metakaolin found by Tscheischwili et al. and in the present work.

Independently, Comeforo, Fischer, and Bradley (1948) recognized that the X-ray diffraction band from metakaolin is 'more distinct than such bands from strictly amorphous solids' and also noted the persistence of external form by use of the electron microscope. They therefore considered that metakaolin had some residual structure and, on the basis of a general comparison of metakaolin with anhydrous pyrophyllite, they considered that 'it does not seem improbable' that there are 'coordinated strings of alumina octahedra, with some buckling of the silica layer'. Roy, Roy, and Francis (1954), using electron microscopy and electron diffraction, have confirmed the persistence of hexagonal morphological form into the metakaolin phase and have observed single-crystal diffractions from the metakaolin in exact agreement with the data for nacrite.

There is abundant evidence, therefore, for the persistence of morpho-

logical form and residual crystalline order in metakaolin. The details of the crystalline order can only be tentatively suggested. Since the alumina layer of the kaolin structure must be modified by the dehydration process, it is reasonable to attribute residual order to the Si–O networks. Brindley and Youell (1951) have shown that when chlorites are subjected to acid attack, the Si–O sheets remain largely intact after the dissolution of the octahedral layers. Of the two suggestions put forward for the arrangement of the Al and O ions in metakaolin, that given by Comeforo et al. is the more plausible, since it is related to structures suggested for aluminium-montmorillonites and for pyrophyllite. In no case, however, is the evidence for the Al–O arrangement very detailed, and for metakaolin the suggestion is little more than a hypothesis. It has, however, been linked up with the process of mullite formation and this will be discussed in later paragraphs.

In concluding this section, it can be said that there is now ample evidence for residual structure in metakaolin most probably associated with the hexagonal Si–O layers. Suggestions which have been put forward regarding the disposition of the Al and O ions are largely unproved hypotheses.

(*b*) *The formation of γ-alumina and mullite.*

The major problem is the nature of the reactions by which these products are formed. Their simultaneous or almost simultaneous appearance in some experiments and the delayed, sometimes long delayed, appearance of mullite in other experiments have been difficult to understand, and although recent investigations have shed light on these apparent anomalies, the problem still is not fully elucidated. Conclusions drawn from a restricted range of observations have frequently been diametrically opposed.

One line of thought, initiated by Comeforo, Fischer, and Bradley (1948), treats the formation of γ-alumina as incidental to the main reaction process. They believed they had evidence from electron microscope observations that mullite needles develop with orientations related to the initial kaolinite flakes and on this basis took the extreme view that 'any γ-alumina which may have been observed in special instances is therefore only incidental and is not a step in the major reaction series of the firing process'. Since γ-alumina has been observed in practically all investigations of fired kaolin minerals and often prior to the formation of mullite, it is a misrepresentation to suggest that it 'may have been observed in special instances'.

The question whether mullite develops with special orientations relative to the parent material is of basic importance. Comeforo et al. regarded the ordered formation of mullite as proceeding from an ordered arrangement of Al octahedra in metakaolin, and subsequent workers (Johns, 1953; Glass, 1954) have developed this line of thought. However, other electron microscope studies by Eitel and Kedesdy (1944) did not show any orientation of the mullite. They obtained very clear micrographs of well-crystallized kaolinite heated progressively to 1200° C. Since the original paper is now almost unobtainable, their own description may usefully be quoted:

'Die bei 950 und 1000 gebrannten Präparate gleichen im wesentlichen der Brennstufe von 900 in der Ausbildung der körnigen Oberflächenstruktur, ohne daß sich irgendeine Orientierung der Teilchen erkennen läßt. Es ist nicht zu bezweifeln, daß hier bereits die ersten Kristallkeime des neugebildeten Mullits vorliegen. Da diese Kriställchen beim Brennen des Kaolins nicht aus der Schmelze entstehen, sondern durch Reaktion im festen Zustand, kann man die bekannte nadelige Form der Mullitkristalle nicht ohne weiteres erwarten. Die tafligen Pseudomorphosen nach Kaolin haben selbst bei einer Exposition der Präparate bei 1100° (Abb. 3) noch einen bemerkenswerten Zusammenhalt. Die Kanten der hexagonalen Formen sind allerdings nicht mehr so scharf, sondern ausgefranst, und besonders fällt auf, daß die vordem so gleichmäßig durchsichtigen Tafeln stofflich auch stark heterogen erscheinen.

Bei 1200° (Abb. 4) sind die großen Tafeln in kleinste Bruchstücke zerfallen, welche völlig körnige Stuktur zeigen. Auffallend sind vor allem die kurzprismatischen Individuen, die auf Mullit hindeuten, sowie deutlich erkennbare reguläre Formen von freier Kieselsäure in Form des Cristobalits.'

Although they observed the persistence of the outlines of kaolinite flakes up to 1100° C., they did not record any oriented development of mullite. Brief reference may be made to a study of muscovite heated to temperatures ranging 1000°–1200° C. by Sundius and Byström (1953). After heating to 1000° C., they observed that 'some of the [mullite] needles were irregularly distributed, but others formed star-shaped aggregates, giving the appearance of a hexagonal pattern'. The situation in muscovite is not exactly the same as that in kaolin minerals and such evidence can be accepted only very tentatively.

However, the ideas advanced by Comeforo et al. have stimulated further investigations into the relation between the crystallinity of kaolin minerals and the formation of mullite. The hypothesis that metakaolin contains 'coordinated strings of alumina octahedra' which can be incorporated easily in a mullite structure suggests that a well-ordered kaolin mineral may form mullite more readily (i.e. at a lower temperature, or in greater quantity) than one with disordered layers. This idea has been developed at length by Johns (1953), and his

experiments together with more extensive investigations by Glass (1954) have yielded results in accord with this general picture. Thus Glass reports that 'the amount of mullite detected at the exothermic peak decreases as the structure becomes more random, and the thermal peak decreases in intensity. The $b_0/3$ shifts in kaolinite evidently cause the development of smaller mullite nuclei with resultant decrease in thermal intensity.'

In the light of these results, a single crystal of nacrite, the best crystallized of all the kaolin minerals and having no admixed impurities, would be expected to reveal most clearly the mode of formation of mullite. The present experiments show that the mullite always forms with random orientation from nacrite. At present there appears to be no other *direct* evidence for the oriented formation of mullite from kaolin minerals than the observations of Comeforo et al. The *indirect* evidence from the work of Johns and of Glass may be capable of an alternative interpretation. It seems very desirable, therefore, that further electron microscope observations should be made and, in particular, a *statistical* assessment of the orientation should be undertaken.

Glass emphasizes that the morphology of kaolin minerals and the presence of mica impurities have marked influences on the development of mullite. It is well established that in the case of halloysite only γ-alumina can be detected in materials heated just beyond the exothermic reaction (Richardson, 1951; Richardson and Wilde, 1952; Glass, 1954). Colegrave and Rigby (1952) quenched material to room-temperature which had been heated in differential thermal apparatus just beyond the exothermic reaction, and they recorded only γ-alumina. Similar experiments by Insley and Ewell (1935) gave the same result; they also showed that by prolonged heating the γ-alumina could be formed at 50° C. lower temperature. Experiments of this kind have led to the conclusion that the exothermic reaction is due to γ-alumina and that 'γ-alumina is the precursor to mullite formation' (Colegrave and Rigby, 1952, p. 366). Comeforo, Fischer, and Bradley (1948) emphasized that the magnitude of the exothermic effect can hardly be attributed to a poorly crystalline phase such as γ-alumina and that it can only arise from the formation of a close-packed phase such as mullite. We agree with this general interpretation, but it is still necessary to explain the apparent absence of mullite after the exothermic effect. In agreement with Glass, we suggest that the mullite nuclei may have formed but not grown to a sufficient size to be observed by X-rays. Glass relates the non-development of the mullite to impedance by γ-alumina. This may

well be true, but a further point for consideration is that poorly crystalline parent material may produce many more nuclei than well crystallized material. A few nuclei may grow to larger size than a large number of competing nuclei. Other examples can be quoted of the slow appearance of a new phase in X-ray diagrams after an exothermic reaction, e.g. the development of olivine from chlorites.

From these considerations of our own work on nacrite and recent investigations of kaolinite and kaolin clays by others, we draw the following conclusions:

(i) At about 900° C. γ-alumina develops from metakaolin with an orientation related to that of the parent mineral. This is made possible by persistence of order through the metakaolin range.

(ii) At about the same temperature or a little higher, mullite nuclei form, giving rise to the exothermic reaction observed thermally. The growth of the mullite nuclei to crystals of a size observable by X-rays seems to depend on the crystallinity of the parent material and of the metakaolin. The mullite develops without preferential orientation which may be related to the nuclei forming when the metakaolin residual structure finally breaks down, i.e. at the time when γ-alumina is forming or has just formed. We agree with Glass that *at this stage* γ-alumina is not part of the main reaction series. Uncombined silica appears to have the cristobalite form.

(iii) The retardation of mullite formation when the parent mineral is disordered seems well established and the data for nacrite fit into the general scheme in this respect.

(iv) At higher temperatures, about 1150° C. in the nacrite experiments, the γ-alumina combines with silica to form further mullite, still with random orientation.

Acknowledgements. –We are indebted to Dr. and Mrs. Roy for permitting one of us (G. W. B.) to see the text of their paper prior to its publication and for permission to make reference to it, and to Dr. Roy and Dr. Eitel for stimulating discussions. One of us (K. H.) is indebted to the Department of Scientific and Industrial Research for a maintenance grant and to the Durham County Education Committee for a post-graduate Scholarship.

References.

Bradley (W. F.) and Grim (R. E.), 1951. High temperature thermal effects of clay and related materials. Amer. Min., vol. 36, pp. 182–201. [M.A. 11-345.]

Brindley (G. W.) and Youell (R. F.), 1951. A chemical determination of 'tetrahedral' and 'octahedral' aluminium ions in a silicate. Acta Cryst., vol. 4, pp. 495–496.

BRINDLEY (G. W.) and OGILVIE (G. J.), 1952. The texture of single crystals of brucite. Acta Cryst., vol. 5, pp. 412–413. [M.A. **12**–208.]

COLEGRAVE (E. B.) and RIGBY (G. R.), 1952. The decomposition of kaolinite by heat. Trans. Brit. Ceram. Soc., vol. 51, pp. 355–367.

COMEFORO (J. E.), FISCHER (R. B.), and BRADLEY (W. F.), 1948. Mullitization of kaolinite. Journ. Amer. Ceram. Soc., vol. 31, pp. 254–259. [M.A. **11**–452.]

EITEL (W.), 1954. The physical chemistry of the silicates. Univ. of Chicago Press. [M.A. **12**–403.]

—— and KEDESDY (H.), 1944. Elektronen-Mikroskopie and -Beugung silikatischer Metaphasen. Vierte Mitt. Der Metakaolin. Abhand. Preuß. Akad. Wiss., Math.-Nat. Kl., Nr. 5, pp. 37–45.

ERVIN (G.), 1952. Structural interpretation of the diaspore–corundum and boehmite–γ-Al_2O_3 transitions. Acta Cryst., vol. 5, pp. 103–108.

GLASS (H. D.), 1954. High-temperature phases from kaolinite and halloysite. Amer. Min., vol. 39, pp. 193–207. [M.A. **12**–491.]

INSLEY (H.) and EWELL (R. H.), 1935. Thermal behaviour of the kaolin minerals. Journ. Res. Nat. Bur. Standards, U.S.A., vol. 14, pp. 615–627.

JOHNS (W. D.), 1953. High-temperature phase changes in kaolinites. Min. Mag., vol. 30, pp. 186–198.

KNORRING (O. von), BRINDLEY (G. W.), and HUNTER (K.), 1952. Nacrite from Hirvivaara, northern Karelia, Finland. Min. Mag., vol. 28, pp. 963–972.

RICHARDSON (H. M.), 1951. Phase changes which occur on heating kaolin clays. Ch. 3, 'X-ray identification and crystal structures of clay minerals'. Mineralogical Society, London. [M.A. **11**–253.]

—— and WILDE (F. G.), 1952. An X-ray study of the crystalline phases that occur in fired clays. Trans. Brit. Ceram. Soc., vol. 51, pp. 387–400.

ROOKSBY (H. P.), 1951. Oxides and hydroxides of aluminium and iron. Ch. X, 'X-ray identification and crystal structures of clay minerals'. Mineralogical Society, London. [M.A. **11**–253.]

ROY (R.), ROY (D. M.), and FRANCIS (E. E.), 1954. New data on the thermal decomposition of kaolinite and halloysite. Paper presented at the 56th Annual Meeting, American Ceramic Society, Chicago.

SUNDIUS (N.), and BYSTRÖM (A. M.), 1953. Decomposition products of muscovite at temperatures between 1000° and 1200° C. Trans. Brit. Ceram. Soc., vol. 52, pp. 632–642.

TSCHEISCHWILI (L.), BÜSSEM (W.), and WEYL (W), 1939. Über den Metakaolin. Ber. Deut. Keram. Gesell., vol. 20, pp. 249–276.

The structure of wadeite.

By D. E. Henshaw.

Department of Physics, University of Western Australia.

[Taken as read January 27, 1955.]

Introduction.

WADEITE has been found only in a suite of leucite-lamproites from the West Kimberley area of Western Australia. The leucite-bearing rocks occur at a number of isolated volcanic vents that have in every instance broken through sedimentary deposits of Permian age.[1] The nature of the mineral, wadeite, has been described by Prider.[2] It is a potassium-zirconium silicate occurring as highly birefringent prisms up to 1 mm. in length with hexagonal-shaped basal sections. It is invariably replaced in part along the poor pyramidal cleavages by calcite. These cleavages, intersecting at angles of nearly 90°, are rendered visible because of the presence of the secondary calcite which has entered along these directions. The mineral is colourless, uniaxial, optically positive, and has ϵ 1·655, ω 1·625, and $\epsilon - \omega$ 0·030. It has a specific gravity of 3·10, is non-magnetic, and insoluble in hot acids. Prider, on the basis of a chemical analysis (table I), calculated the formula to be

$$K_{2\cdot05}(Ca,Na)_{0\cdot95}(Zr,Ti,Al)_{1\cdot23}(Si,P,Al)_{4\cdot00}O_{12}.$$

X-ray powder and Laue diffraction work, carried out in this department by Shearer, Robinson, and Jefferies,[3] showed the diffraction symmetry to be $6/m$ (C_{6h}) and the unit-cell dimensions to be a 6·89 and c 10·18 Å. On the basis of this information and the chemical data, the formula ascribed to wadeite was $(K(Zr,Ca)Si_2O_6)_3$. The purpose of the present work was to confirm these earlier observations and to attempt a complete structure determination of what appeared to be a unique mineral structure.

[1] A. Wade and R. T. Prider, Quart. Journ. Geol. Soc. London, 1940, vol. 96, p. 39. [M.A. 8–28.]

[2] R. T. Prider, Min. Mag., 1939, vol. 25, p. 379.

[3] J. Shearer, E. T. Robinson, and J. T. Jefferies, Min. Mag., 1952, vol. 29, Proc. p. lxi.

TABLE I. Chemical analysis of wadeite.

	Molecular proportions (Prider).	No. of metal atoms on basis of 18(O).	Valency.	Ionic radii (Å.).	Grouping.
P_2O_5	0·022	0·34	5	0·34	6(Si,Al,P)$^{4+}$
SiO_2	0·657	5·06	4	0·39	
Al_2O_3	0·059	0·91	3	0·57	
MgO	0·007	0·06	2	0·78	2(Zr,Ti,Mg,Al,Na)$^{4+}$
TiO_2	0·020	0·15	4	0·64	
ZrO_2	0·173	1·33	4	0·87	
Na_2O	0·045	0·69	1	0·98	
CaO	0·093	0·73	2	1·06	4(K,Ca,Ba,Na)$^{+}$
K_2O	0·196	3·02	1	1·33	
BaO	0·008	0·06	2	1·43	
		12·35			
Oxygen		18	−2	1·32	18O^{2-}

EXPERIMENTAL.

The crystal used was of the shape and size shown in fig. 1. The direction of the *c*-axis was reasonably well defined but there was only one 120° interfacial angle that could be distinguished.

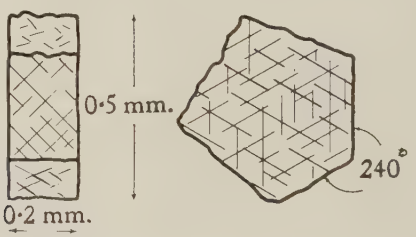

FIG. 1. Size of the crystal used and general appearance of the cleavage cracks.

Single-crystal oscillation and Weissenberg diffraction patterns were prepared using copper and molybdenum $K\alpha$ radiations. The unit-cell dimensions were determined by the θ-method[1] to be a 6·893 ± 0·004 Å and c 10·172 ± 0·002 Å. The intensities of the X-ray reflections were estimated visually on a series of Weissenberg photographs and the appropriate absorption, Lorentz, and polarization corrections were applied. The observed structure amplitudes (F_0) so obtained are listed in tables II and III. In order to check the accuracy of the visual estimation of intensity, a number of reflection intensities were measured on a Geiger-counter spectrometer. As can be seen from table IV, the agree

[1] O. Weisz, W. Cochran, and W. F. Cole, Acta Cryst., 1948, vol. 1, p. 83. [M.A.

ment is quite reasonable, except for some of the weaker reflections and the strong reflection ($2\bar{1}\bar{1}2$). Inaccuracy in the visual method is to be expected for such very strong and weak reflections.[1]

TABLE II. Observed and calculated structure amplitudes F($hki0$).

h	k	i	l.	F_o.	F_c.	h	k	i	l.	F_o.	F_c.
0	0	0	0	—	356	5	3	$\bar{8}$	0	35	36
1	0	$\bar{1}$	0	—	41	6	2	$\bar{8}$	0	10	13
2	$\bar{1}$	$\bar{1}$	0	68	68	7	1	$\bar{8}$	0	37	37
2	0	$\bar{2}$	0	< 8	7	8	0	$\bar{8}$	0	50	46
3	$\bar{1}$	$\bar{2}$	0	42	48	9	$\bar{1}$	$\bar{8}$	0	22	18
4	$\bar{2}$	$\bar{2}$	0	81	86	10	$\bar{2}$	$\bar{8}$	0	23	29
2	1	$\bar{3}$	0	< 5	7	11	$\bar{3}$	$\bar{8}$	0	< 11	1
3	0	$\bar{3}$	0	95	95	12	$\bar{4}$	$\bar{8}$	0	< 11	8
4	$\bar{1}$	$\bar{3}$	0	75	80	13	$\bar{5}$	$\bar{8}$	0	< 11	8
5	$\bar{2}$	$\bar{3}$	0	8	9	5	4	$\bar{9}$	0	40	32
6	$\bar{3}$	$\bar{3}$	0	46	51	6	3	$\bar{9}$	0	56	60
3	1	$\bar{4}$	0	< 6	3	7	2	$\bar{9}$	0	< 9	1
4	0	$\bar{4}$	0	38	40	8	1	$\bar{9}$	0	< 10	3
5	$\bar{1}$	$\bar{4}$	0	65	67	9	0	$\bar{9}$	0	27	28
6	$\bar{2}$	$\bar{4}$	0	31	28	10	$\bar{1}$	$\bar{9}$	0	< 11	5
7	$\bar{3}$	$\bar{4}$	0	37	36	11	$\bar{2}$	$\bar{9}$	0	< 11	5
8	$\bar{4}$	$\bar{4}$	0	48	50	12	$\bar{3}$	$\bar{9}$	0	< 11	14
3	2	$\bar{5}$	0	13	$\bar{12}$	13	$\bar{4}$	$\bar{9}$	0	22	11
4	1	$\bar{5}$	0	106	111	6	4	$\bar{10}$	0	< 10	4
5	0	$\bar{5}$	0	33	27	7	3	$\bar{10}$	0	< 10	0
6	$\bar{1}$	$\bar{5}$	0	25	19	8	2	$\bar{10}$	0	28	34
7	$\bar{2}$	$\bar{5}$	0	60	60	9	1	$\bar{10}$	0	< 11	3
8	$\bar{3}$	$\bar{5}$	0	< 8	7	10	0	$\bar{10}$	0	< 11	5
9	$\bar{4}$	$\bar{5}$	0	< 9	1	11	$\bar{1}$	$\bar{10}$	0	30	29
10	$\bar{5}$	$\bar{5}$	0	18	24	12	$\bar{2}$	$\bar{10}$	0	< 12	11
4	2	$\bar{6}$	0	21	14	13	$\bar{3}$	$\bar{10}$	0	< 12	0
5	1	$\bar{6}$	0	33	23	6	5	$\bar{11}$	0	< 11	2
6	0	$\bar{6}$	0	33	37	7	4	$\bar{11}$	0	16	26
7	$\bar{1}$	$\bar{6}$	0	< 8	4	8	3	$\bar{11}$	0	15	12
8	$\bar{2}$	$\bar{6}$	0	< 8	2	9	2	$\bar{11}$	0	21	23
9	$\bar{3}$	$\bar{6}$	0	42	45	10	1	$\bar{11}$	0	< 11	18
10	$\bar{4}$	$\bar{6}$	0	18	14	11	0	$\bar{11}$	0	< 11	1
11	$\bar{5}$	$\bar{6}$	0	15	12	12	$\bar{1}$	$\bar{11}$	0	< 12	9
12	$\bar{6}$	$\bar{6}$	0	32	29	7	5	$\bar{12}$	0	18	12
4	3	$\bar{7}$	0	16	17	8	4	$\bar{12}$	0	< 11	6
5	2	$\bar{7}$	0	39	51	9	3	$\bar{12}$	0	25	30
6	1	$\bar{7}$	0	< 8	3	10	2	$\bar{12}$	0	< 12	9
7	0	$\bar{7}$	0	23	22	11	1	$\bar{12}$	0	< 12	0
8	$\bar{1}$	$\bar{7}$	0	51	65	12	0	$\bar{12}$	0	15	18
9	$\bar{2}$	$\bar{7}$	0	< 9	8	7	6	$\bar{13}$	0	< 12	0
10	$\bar{3}$	$\bar{7}$	0	23	15	8	5	$\bar{13}$	0	< 12	13
11	$\bar{4}$	$\bar{7}$	0	28	32	9	4	$\bar{13}$	0	< 12	4
12	$\bar{5}$	$\bar{7}$	0	< 11	10	10	3	$\bar{13}$	0	< 12	1
13	$\bar{6}$	$\bar{7}$	0	< 12	6						

[1] W. Cochran, Acta Cryst., 1950, vol. 3, p. 268

TABLE III. Observed and calculated structure amplitudes F(2$\bar{h}\bar{h}hl$).

The letter d indicates that the reflection could be detected but not measured.

$$R = (F_c - F_0)/F_c$$

h	l.	F_0.	F_c.	R.	h	l.	F_0.	F_c.	R.
0	0	—	356	—	4	15	—	$\bar{1}$	—
0	2	—	9	—	4	16	—	26	—
0	4	77	82	0·06	4	17	—	1	—
0	6	61	$\bar{6}4$	0·05	4	18	—	16	—
0	8	91	87	0·05	4	19	—	$\bar{1}$	—
0	10	d	$2\bar{0}$	—	6	0	47	52	0·10
0	12	45	41	0·10	6	1	—	$\bar{3}$	—
0	14	—	$\bar{8}$	—	6	2	64	58	0·10
0	16	55	54	0·02	6	3	23	20	0·15
0	18	d	18	—	6	4	33	39	0·15
0	20	d	21		6	5	d	$\bar{1}\bar{5}$	—
2	0	63	68	0·07	6	6	32	22	0·45
2	1	50	$\bar{4}\bar{3}$	0·16	6	7	—	0	—
2	2	103	110	0·06	6	8	—	$\bar{1}\bar{2}$	—
2	3	19	$\bar{1}\bar{9}$	0·00	6	9	—	$\bar{6}$	—
2	4	59	54	0·09	6	10		5	—
2	5	—	$\bar{2}$	—	6	11	—	12	
2	6	50	41	0·22	6	12	—	14	—
2	7	35	32	0·09	6	13	—	4	—
2	8	—	$\bar{1}\bar{3}$	—	6	14	—	24	—
2	9	d	$\bar{1}\bar{4}$	—	6	15		$\bar{1}$	
2	10	d	14	—	6	16		18	—
2	11		$\bar{3}$	—	6	17	—	$\bar{4}$	—
2	12		14	—	6	18	—	14	
2	13		$\bar{8}$	—	8	0	51	50	0·02
2	14	—	37	—	8	1	—	$\bar{3}$	—
2	15	—	12	—	8	2	59	57	0·04
2	16	—	23	—	8	3	—	3	—
2	17	—	$\bar{1}$	—	8	4	—	5	—
2	18	—	22	—	8	5	—	$\bar{3}$	—
2	19		$\bar{2}$	—	8	6	d	18	—
2	20		13	—	8	7	—	2	—
4	0	78	86	0·09	8	8	—	$\bar{4}$	—
4	1	—	4	—	8	9		$\bar{2}$	—
4	2	58	63	0·08	8	10	—	16	—
4	3	—	4	—	8	11	—	1	—
4	4	65	59	0·10	8	12	—	$\bar{1}$	—
4	5	—	3	—	8	13	—	0	—
4	6	d	13		8	14	—	15	—
4	7	—	$\bar{2}$	—	8	15		0	—
4	8	—	9	—	8	16	—	14	—
4	9	—	1	—	10	0	22	24	0·08
4	10	—	6		10	1	—	11	—
4	11	—	$\bar{1}$	—	10	2	35	41	0·15
4	12	—	24	—	10	3	—	$\bar{1}\bar{6}$	—
4	13	—	1	—	10	4	—	13	—
4	14	—	24	—	10	5	—	12	—

TABLE III (*contd.*)

h	l.	F_o.	F_c.	R.	h	l.	F_o.	F_c.	R.
10	6	—	17	—	12	1	—	$\bar{5}$	—
10	7	—	$\bar{7}$	—	12	2	—	21	—
10	8	—	$\bar{8}$	—	12	3	—	5	—
10	9	—	8	—	12	4	—	12	—
10	10	—	6	—	12	5	—	$\bar{4}$	—
10	11	—	$\bar{8}$	—	12	6	—	2	—
10	12	—	4	—	12	7	—	4	—
10	13	—	5	—	12	8	—	20	—
10	14	—	16	—	12	9	—	$\bar{4}$	—
12	0	31	29	0·07	12	10	—	1	—

TABLE IV. Comparison of counter intensities (I_c) with visual intensities (I_v).

h	k	i	l.	I_c.	I_v.	h	k	i	l.	I_c.	I_v.
4	$\bar{2}$	$\bar{2}$	0	51	51	0	0	0	8	36	36
6	$\bar{3}$	$\bar{3}$	0	12	10	0	0	0	10	6	—
8	$\bar{4}$	$\bar{4}$	0	10	8	0	0	0	12	6	3
10	$\bar{5}$	$\bar{5}$	0	1·2	0·8	0	0	0	16	6	4·5
12	$\bar{6}$	$\bar{6}$	0	1·8	1·9	2	$\bar{1}$	$\bar{1}$	2	152	133
0	0	0	4	50	50	4	$\bar{2}$	$\bar{2}$	4	28	32
0	0	0	6	21	21	6	$\bar{3}$	$\bar{3}$	6	4	3·5

An interesting feature of the oscillation photographs was the occurrence of a number of powder diffraction lines superimposed on the single crystal pattern. Reference to the American Society for Testing Materials index showed that the spacings of these lines corresponded to those of calcite, thus confirming the presence of this mineral in the surface cracks of the crystal.

SOLUTION OF STRUCTURE.

Examination of the zero-level and first-level Weissenberg photographs of the crystal taken with the c-axis and the $(2\bar{1}\bar{1}0)$-axis (perpendicular to the a- and c-axes) as the axes of rotation, confirmed the diffraction symmetry of $6/m$ (C_{6h}). This, together with the systematically absent reflections, $000l$ when l is odd, indicated that wadeite belongs either to the space group $P6_3$ (C_6^6) or $P6_3/m$ (C_{6h}^2).

Consideration of the unit-cell dimensions and the measured density shows there is one molecule, containing eighteen oxygen atoms, per unit cell (table I). Furthermore, general considerations of symmetry and chemical data, together with the failure of tests for non-centrosymmetry, suggest the formula to be $Zr_2K_4Si_6O_{18}$ and that it belongs to the $P6_3/m$ (C_{6h}^2) space group. It is obvious from table I that this is only an idealized formula, since there has been considerable substitution of the metal atoms.

It has been noted that the cleavage cracks in the prism faces of the

crystal cross at nearly 90°. This is a typical property of pyroxen which have, in general, a somewhat similar type of chemical formula wadeite. However, it is impossible to fit a pyroxene type of silicon oxygen chain into the symmetry of the $P6_3/m$ space group.

Wadeite, then, appears to be based on a silicon-oxygen framework six silicon and eighteen oxygen atoms in the unit cell. By constructi a model of wooden spher representing oxygen aton within the confines of a unit ce of appropriate dimensions, it wa found that there were two, no very different, frameworks tha fulfilled the required symmetr conditions. The structure base on either of these two frame works defined the x, y co ordinates of the zirconium an potassium atoms; i.e. (0,0,z) for zirconium and (2/3,1/3,z) and (1/3,2/3,z for potassium.

Fig. 2. Form of the temperature factor plotted against $(\sin\theta)/\lambda$.

Two heavy atoms, such as zirconium, at the origin of the two dimensional projection along the c-axis, provide a large, positive contri bution to the structure factors corresponding to reflections of the typ ($hki0$). There would therefore be very few errors in assuming all thes structure factors to be positive. A Fourier synthesis of this projectio was carried out using the values of F_0 in table II and taking them all t be positive. This synthesis showed the positions of all the atoms excep for six oxygens, and established which of the two model structures wa to be accepted.

In order to calculate the structure factors from atomic co-ordinate it is necessary to know the atomic scattering factors for the ator involved. For silicon and oxygen, these are listed in available table However, reference to the chemical data in table I shows that the natu of the other atoms in a unit cell is varied. A weighted mean of th atomic weights of the elements likely to be in the 'potassium' positio corresponded closely to that of potassium, whose f_0 values are give directly in the tables. A similar mean for the 'zirconium' positio suggested a quadruply-ionized element of atomic number 36. It w therefore necessary to construct an atomic scattering factor curv appropriate to this average atomic number. The values given in table have been derived from those of bromine (35) and rubidium (37).

TABLE V. Atomic scattering factor f_0 for 'Zr^{4+}'.

$\sin\theta/\lambda$	0·0	0·1	0·2	0·3	0·4	0·5	0·6	0·7	0·8	0·9	1·0
f_0	...	32·0	31·2	28·4	24·5	21·1	18·7	16·6	14·6	12·8	11·2	9·9

Refinements were made to the atomic parameters given by the model, using trial and error methods, until the best agreement was obtained

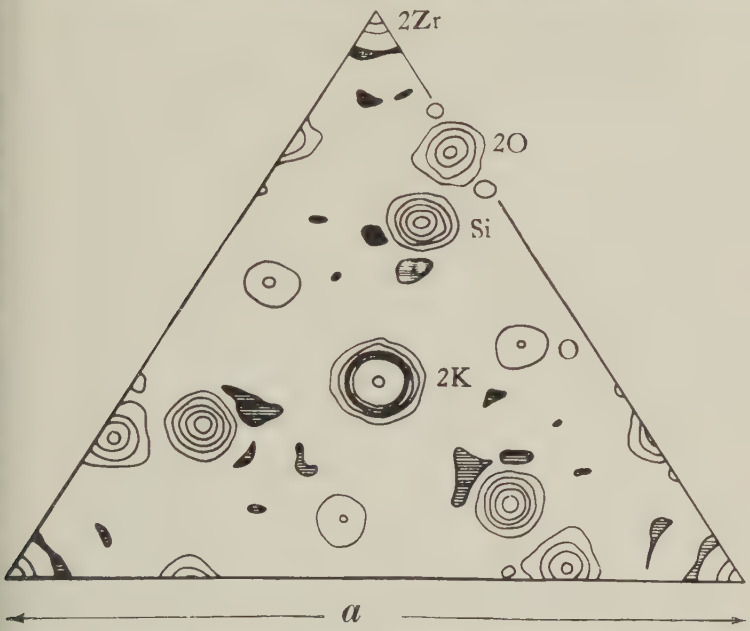

FIG. 3. Projection of electron density along the c-axis of wadeite. The contours are at the arbitrary levels of 0, 1, 2, 3, 4, 5, 10, except at the three zirconium positions where they are at 0, 10, and 20.

between observed and calculated values of the structure factors. The original values of the calculated structure factors had to be multiplied by a factor to reduce their numerical values to the arbitrary scale of the observed structure factors. This factor consists of a constant times the temperature factor. The experimentally determined curve (fig. 2), which includes a small absorption component, corresponds reasonably well to an exponential temperature factor of the form $e^{-B\sin^2\theta}$, where $B = 0{\cdot}35$. Final values of F_c are listed in table II.

A two-dimensional Fourier synthesis was carried out using reflections of the form $(hki0)$; the result is shown in fig. 3. All values of F_0 up to $\sin\theta/\lambda = 1$ were used and where these were not observed, owing

to their low intensity, calculated values were substituted. The projection substantially confirms x- and y-co-ordinates listed in table VI although it suggests (0·387,0·256,z) and (0·258,0·236,z) might be more appropriate for the silicon position and the general oxygen position respectively. Adoption of these values does not, however, improve the agreement of F_0 and F_c.

For the second set of reflections investigated ($2h\bar{h}\bar{h}l$), only 19 significant observed structure factors could be measured out of a total of 108. This is somewhat unsatisfactory and the usefulness of a Fourier projection would be very doubtful. Nevertheless, the agreement obtained, as indicated by $R = (F_c - F_0)/F_c$ in table III, is sufficient to verify the structure already postulated. There is one serious difference between F_0 and F_c for ($6\bar{3}\bar{3}6$), but this is a relatively weak reflection and thus liable to a large error in measurement. It must be noted that the calculated structure factors for the ($2h\bar{h}\bar{h}l$) reflections as listed in table III have involved the use of the correlating factor derived experimentally for the ($hki0$) reflections. This is strictly not justified, since the temperature factor will not be the same in all directions in the wadeite crystal, but the error will not affect the results. The final values for all the atomic co-ordinates are tabulated in table VI.

Table VI. Co-ordinates of the atoms of wadeite expressed as fractions of a, a and c.

12O	(0·263	0·236	0·114)	(0·764	0·027	0·114)	(0·973	0·737	0·114
	(0·737	0·764	0·886)	(0·236	0·973	0·886)	(0·027	0·263	0·886
	(0·737	0·764	0·664)	(0·236	0·973	0·664)	(0·027	0·263	0·664
	(0·263	0·236	0·386)	(0·764	0·027	0·386)	(0·973	0·737	0·386
6O	(0·500	0·100	0·250)	(0·900	0·400	0·250)	(0·600	0·500	0·250
	(0·500	0·900	0·750)	(0·100	0·600	0·750)	(0·400	0·500	0·750
6Si	(0·389	0·255	0·250)	(0·745	0·134	0·250)	(0·866	0·611	0·250
	(0·611	0·745	0·750)	(0·255	0·866	0·750)	(0·134	0·389	0·750
4K	(0·666̂	0·333̂	0·558)	(0·666̂	0·333̂	0·942)	—	—	—
	(0·333̂	0·666̂	0·442)	(0·333̂	0·666̂	0·058)	—	—	—
2Zr	(0	0	0)	(0	0	0·500)			

Description of structure.

The structure of wadeite is based on a framework of silica tetrahedra, the potassium and zirconium atoms fitting into the interstices. The fundamental unit of this framework is the $(Si_3O_9)^{6-}$ group (fig. 4), two of which combine with $4K^{+}$ and $2Zr^{4+}$ to form the neutral contents of

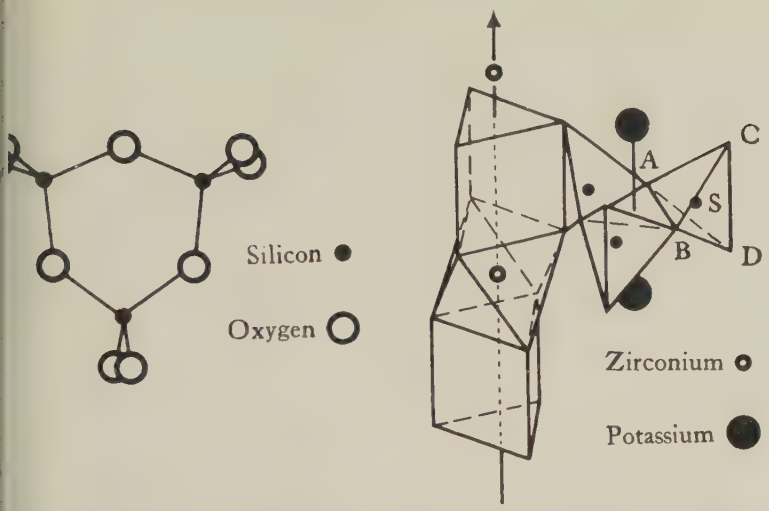

FIG. 4. The $(Si_3O_9)^{6-}$ unit, which consists of three silicon-oxygen tetrahedra ming a ring.

FIG. 5. Arrangement of the metal atoms within the silicon-oxygen framework. ne oxygen atoms are at the corners of the figure.

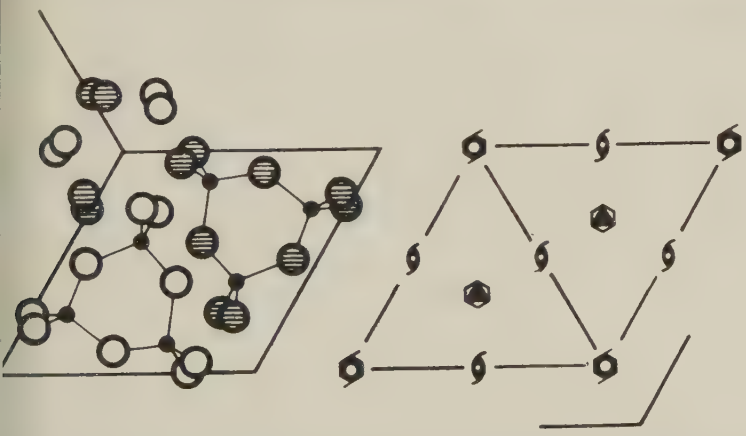

Fig. 6. Grouping of the $(Si_3O_9)^{6-}$ units in the unit cell and the symmetry elements the $P6_3/m$ space group. The shaded groups are separated from the unshaded by screw component of $c/2$.

ne unit cell. The $(Si_3O_9)^{6-}$ groups are arranged about the hexad screw xis as illustrated in fig. 5.

The oxygen atoms are grouped in the manner indicated in fig. 5, here an oxygen atom is situated at each corner of the figure. The

zirconium atom is then situated at the centre of the octahedron form
by the six oxygen atoms; i.e. at the positions (0,0,0) and (0,0,$\frac{1}{2}$). Mir
reflection planes intersect the hexad screw axis (6_3) at $z = \frac{1}{4}$ a
$z = \frac{3}{4}$, perpendicularly between the octahedra. The $(Si_3O_9)^{6-}$ groups
in these planes with a potassium atom symmetrically above and bel
the centre of each.

From the co-ordinates listed in table VI, it was possible to calcula
the interatomic distances. The values obtained for the O–O distan
in the silica tetrahedra (fig. 5) are: $AB = 2{\cdot}49$, $AC = AD = 2{\cdot}$
$BC = BD = 2{\cdot}53$, $CD = 2{\cdot}77$ Å. The average of these is 2·60 Å
which is the generally accepted O–O bond distance in these tetrahed
Although the maximum error in these distances is 0·1 Å., the value
CD is still significantly large.

The Si–O distances obtained are: $SA = 1{\cdot}60$, $SB = 1{\cdot}58$, $SC =$
$SD = 1{\cdot}60$ Å. The accepted value[1] is 1·60 Å. and the close agreeme
of the measured bond lengths tends to support the large O–O distan
quoted for CD. The Zr–O distance is 2·07 Å. Goldschmidt radii f
zirconium and oxygen would suggest this value to be about 2·17 Å. Th
K–K distance was found to be 3·30 Å. as compared with Goldschmidt
distance of about 2·7 Å. Each potassium atom is surrounded by nin
oxygen atoms; three at a distance of 2·82, three at 3·06, and three
3·44 Å. Goldschmidt radii suggest that these figures could be as lo
as 2·65 Å.

Conclusion.

The complete structure of wadeite has been determined by X-ra
methods. It has the space group, $P6_3/m$, unit-cell dimensions

$$a\ 6{\cdot}893 \pm 0{\cdot}004, \qquad c\ 10{\cdot}172 \pm 0{\cdot}002\ \text{Å.},$$

and may be represented ideally by the formula $Zr_2K_4Si_6O_{18}$.

The fundamental structural unit is the $(Si_3O_9)^{6-}$ silicon-oxygen rin
The only previously known silicate mineral to be built up on this un
is benitoite[2] from San Benito County, California, having the formu
$BaTiSi_3O_9$ and space group $P\bar{6}c2$ (D^2_{3h}).

There is evidence of some distortion in the individual silica tetrahedr
This distortion causes two-thirds of the oxygen atoms in wadeite to l
closer to the positively charged zirconium and potassium ions tha

[1] J. V. Smith, Acta Cryst., 1954, vol. 7, p. 479. [M.A. **12**–430.]
[2] W. H. Zacharisen, Zeits. Krist., 1930, vol. 74, p. 139. [M.A. **4**–367.]

would be the case for regular tetrahedra, and yet it does not alter the Si–O distances or the average O O distances in each tetrahedron.

Acknowledgements. The author is indebted to Professor R. T. Prider who supplied the crystal of wadeite, to Mr. G. B. Robertson whose Geiger-counter equipment was used, to Mr. J. Shearer for helpful advice, and in particular to Professor C. J. B. Clews for his patient and helpful supervision. The work was made possible by a grant from the University Research Grants Committee.

Australites from Harrow, Victoria.

By George Baker, M.Sc.

Department of Geology, Melbourne University, Australia.

[Taken as read January 27, 1955.]

THIRTY-FOUR specimens of australites were collected by Miss J Jones and her brother Mr. Jones, during forty years while work on their property of 2000 acres, on the north bank of the Glenelg riv This is situated 3½ miles due east of Harrow (37° 8′ S., 141° 33′ E.) the western district of Victoria, 236 miles north of west of Melbourn The collection was kindly submitted for examination through Mr. E. Gill of the National Museum, Melbourne.

The greater proportion (60 %) of the specimens in the collecti consists of australite cores, the remainder being button-, lens-, boat and dumb-bell-shaped forms. Many are relatively well preserved, a fe have been abraded. The total weight of australite glass represented these specimens amounts to 305·05 grams, and the average specif gravity of the thirty-four specimens is 2·42.

Three alien specimens accompanied the collection of australite One is a waterworn pebble of basalt with a specific gravity value 3·08, which shows evidence of smoothing on one edge, evidently b aborigines. It is therefore surmised that this specimen was carried in the area by human agency. The other two alien specimens are abrad pebbles of smoky quartz (var. morion) having specific gravity values 2·60 and 2·66, both of which are significantly greater than the speci gravity values of the australites. Thin splinters of these specimens a birefringent and uniaxial positive. They were also probably carri into the area by aborigines.

Two specimens of australites removed from the collection prior this investigation are reported to be of the large dumb-bell type. T area upon which the australites were discovered consists typically thick, red-coloured clayey soils.

Where not abraded, the australites display the characteristic flo lines, pits, and grooves found on most relatively well-preserved spe mens from various parts of Australia. Some of the grooves have be

eepened and widened by natural etching and infilled with hard, emented clay derived from the surface materials on which the australites lay.

The weight, specific gravity, dimensions, and radii of curvature of the osterior (R_B) and anterior (R_F) surfaces of each australite in the collection are listed in table I.

ABLE I. Weight, specific gravity, dimensions, and radii of curvature of australites from Harrow.

o.	Shape type.	Weight gm.	Sp. gr.	Depth mm.	Diameter mm.	Width mm.	Length mm.	R_B mm.	R_F mm.
	Button	3·914	2·420	11	17	—	—	9	11·5
	,,	5·892	2·407	13	19	—	—	9·5	13
	,,	5·370	2·413	12	21	—	—	13	12
	,,	3·305	2·419	11	22	—	—	12·5	15
	,,	2·339	2·431	9	16·5	—	—	10	10
	,,	2·166	2·432	7	18	—	—	14	14
	Lens	2·873	2·403	7·5	18	—	—	11·5	13·5
	,,	2·783	2·415	9	17	—	—	10	11
	,,	1·812	2·436	6	15·5	—	—	11	11
	,,	1·230	2·453	7	12	—	—	6·5	8·5
	Boat	3·477	2·418	9	—	14	23	7* / 20·5**	7* / 14·5**
	Dumb-bell	4·286	2·419	7	—	12	23	6*	9*
	,,	4·406	2·429	7	—	13	36	6·5*	8·5*
	,,	29·528	2·421	16	—	21	64	11*	11*
	Round core	5·384	2·440	14	17	—	—	13	12
	,,	5·880	2·423	15·5	19·5	—	—	14·5	13·5
	,,	6·180	2·418	14	20	—	—	17·5	11
	,,	6·583	2·411	12·5	21	—	—	19	14
	,,	8·188	2·411	14·5	22·5	—	—	18·5	14·5
	,,	8·628	2·468	13	21·5	—	—	20	16
	,,	13·402	2·413	17·5	26	—	—	17·5	15·5
	,,	14·471	2·422	16	27	—	—	22	20
	,,	17·833	2·401	18·5	29	—	—	21·5	19·5
	,,	30·765	2·406	25·5	32	—	—	20	17·5
	Oval core	13·084	2·428	17·5	—	23·5	26·5	17·5* / 23·5**	17·5* / 17·5**
	,,	14·352	2·386	18·5	—	25	28·5	20* / 19**	13* / 15·5**
	,,	33·782	2·426	22	—	34	36	26* / 29·5**	24* / 25·5**
	Fragment of elongated core	2·396	2·446	—	—	—	27	—	—
	Elongated core	4·087	2·425	12·5	—	13	22	25	16·5
	,,	5·360	2·402	13	—	14·5	24	25	25·5
	,,	7·504	2·401	15	—	17·5	25	19	16·5
	,,	8·847	2·396	14	—	20	29·5	13* / 33·5**	11* / 33**
	,,	11·385	2·408	17·5	—	18	28·5	23	25·5
	,,	12·775	2·438	16	—	23	29·5	17* / 25**	15·5* / 27·5**

Measurements of the dimensions and radii of curvature listed in table I ave been determined to the nearest 0·5 mm. In the R_B and R_F columns he asterisks connote values of the radii of curvature across the widths f the bulbous ends of the dumb-bells. Where two values are given for

each of R_B and R_F of the boat, oval core, and elongated core types australites, the first figure (one asterisk) refers to the radius of curvatu across the width, while the second and usually larger figure (tw asterisks) refers to the radius of curvature along the length.

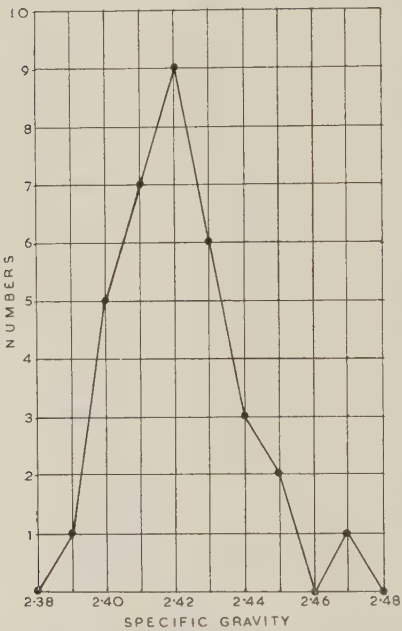

Fig. 1. Frequency diagram showing distribution of specific gravity values of australites from Harrow.

The specific gravity valu were determined on an ai damped balance at 16° C. b Mr. G. C. Carlos. The aver specific gravity of 2·42 for t collection has been dete mined from values rangi from 2·386 (for an oval core) 2·468 (for a round core). Th lower value of 2·386, which w checked and re-checked, is ev dently due to the presence a few gas bubbles of small siz The distribution of the specif gravity values is shown by t frequency diagram (fig. 1), whe the mode is 2·42, thus agreei with the calculated mean specif gravity.

The width values listed f the dumb-bell-shaped australit (table I) refer to their bulbo ends; the constricted wai regions were not measured.

The depth, diameter, width, length, and radii of curvature measu ments were obtained from silhouette tracings of each form. Rotati of the round-form specimens in a beam of light revealed their symmet about the polar axis; for in the 45° and 90° positions their silhouett matched those of the original position from which the silhouette traci were made.

The values for the radii of curvature of posterior (R_B) and anteri (R_F) surfaces were obtained from the silhouette tracings by constructi three chords for each curved surface and bisecting these chords. Norm to the chords through the bisectrices met in three-point intersections occasionally with a small triangle of error. Since the silhouettes we traced at magnifications of 5·5 times, the triangles of error were n

ligible. The points of intersection were used as the foci for the construction of circles about each surface tracing. For all the round forms of the australites from Harrow it was found that the arcs of curvature of both the posterior and the anterior surfaces were coincident with portions of the arcs of curvature of the constructed circles. The curvature of each surface occupied approximately 25 % to 30 % of the arc of curvature of each circle. The same applied to silhouettes constructed in similar manner parallel with the shorter diameter (i.e. width) of all the elongated australites in the collection, but not always to those constructed parallel with the longer diameter (i.e. length), where it was found that the arc of curvature was flatter in the polar regions, steeper in equatorial regions. This indicates that the elongated australites were derived from slightly flattened original spheroids or ellipsoids, while the round forms of australites were evidently derived from original spheres.

The relationships between R_B and R_F, for values determined on round forms and values determined across the shorter diameters of elongated forms, are shown by the scatter diagram, fig. 2. It is observed from fig. 2 that there is a general increase of R_F, with increasing R_B from shape type to shape type.

The ranges in values and average values determined for the dimensions and radii of curvature of the australites are set out in tables II and III.

Comparisons of the values listed in tables II and III reveal that the australites from Harrow show the following features:

(1) Buttons are heavier (and larger) than lenses and heavier than the only boat-shaped specimen in the collection, but lighter (and smaller) than the dumb-bells, round cores, and elongated cores.

(2) The specific gravity values are uniform from shape type to shape type, with the average for lenses only 0·01 in excess of the averages for the other shape types. Consequently the frequency diagram (fig. 1), embracing the specific gravity values of all the shape types represented, reveals a relatively even distribution.

(3) The larger the dimensions of the australites, the greater becomes their individual weight, but there is nevertheless relative constancy of specific gravity, indicating that the source material must have been a well-mixed, more or less homogeneous substance.

(4) The depth values for all shape types increase from lenses, through buttons and dumb-bells to round and elongated cores.

(5) The diameter values of the round forms increase from lenses, through buttons to round cores.

TABLE II. Ranges in values for complete or nearly complete australites from Harrow.

Shape type.	Weight gm.	Sp. gr.	Depth mm.	Diameter mm.	Width mm.	Length mm.	R_B mm.	R_F mm.
Buttons ...	2·17 to 5·89	2·41 to 2·43	7 to 13	16·5 to 22	—	—	9 to 14	10 to 15
Lenses ...	1·23 to 2·87	2·40 to 2·45	6 to 9	12 to 18	—	—	6·5 to 11·5	8·5 to 13·5
Boat	3·48	2·42	9	—	14	23	7* 20·5**	7* 14·5**
Dumb-bells ...	4·29 to 29·53	2·42 to 2·43	7 to 16	—	12 to 21	23 to 64	6 to 11*	9 to 11*
Round cores ...	5·38 to 30·77	2·40 to 2·47	12·5 to 26·5	17 to 32	—	—	13 to 22	11 to 20
Elongated cores ...	4·09 to 33·78	2·39 to 2·45	12·5 to 22	—	13 to 34	22 to 36	13 to 26* 19 to 33·5**	11 to 25·5* 15·5 to 33**
Totals ...	1·23 to 33·78	2·39 to 2·47	6 to 25·5	12 to 32	12 to 34	22 to 64	6·5 to 26*	7 to 25·5*

* and **—as for comments on table I.

Total weight of all specimens = 305·05 gm.

TABLE III. Average values for complete or nearly complete australites from Harrow.

Shape type.	Weight gm.	Sp. gr.	Depth mm.	Diameter mm.	Width mm.	Length mm.	R_B mm.	R_F mm.
Buttons	3·99	2·42	10·5	18	—	—	11·5	12·5
Lenses	2·38	2·43	7	15	—	—	10	11
Boat	3·48	2·42	9	—	14	23	7* 20·5**	7* 14·5**
Dumb-bells ...	12·74	2·42	9·5	—	14	41	8*	9·5*
Round cores ...	11·73	2·42	15·5	22·5	—	—	18·5	15·5
Elongated cores	12·35	2·42	14·5	—	19·5	27	20·5* 26**	18·5* 24**
Total average ...	8·97	2·42	13	19·5	17·5	29·5	—	—

* and **—as for comments on table I.

(6) The width values of elongated forms increase from boats, through dumb-bells to elongated cores.

(7) The length values of the elongated forms increase from boats, through elongated cores to dumb-bells.

(8) There is an increase in depth with increase in diameter among the round forms, and an increase in depth with increase in width and length among the elongated forms.

(9) Width increases as the length increases in the elongated forms.

(10) Whereas R_F is slightly greater in value than R_B for buttons and lenses, the reverse applies to the round cores (cf. scatter diagram, fig. 2). This means that the arc of curvature of anterior surfaces is a little flatter than that of posterior surfaces of buttons and lenses, but steeper for round cores.

Such effects as those indicated in item (10) arise from greater degrees

of ablation of the front surfaces of buttons and lenses in proportion to the sizes of the primary forms (spheres) from which they were derived, compared to the primary forms (larger spheres) from which the round

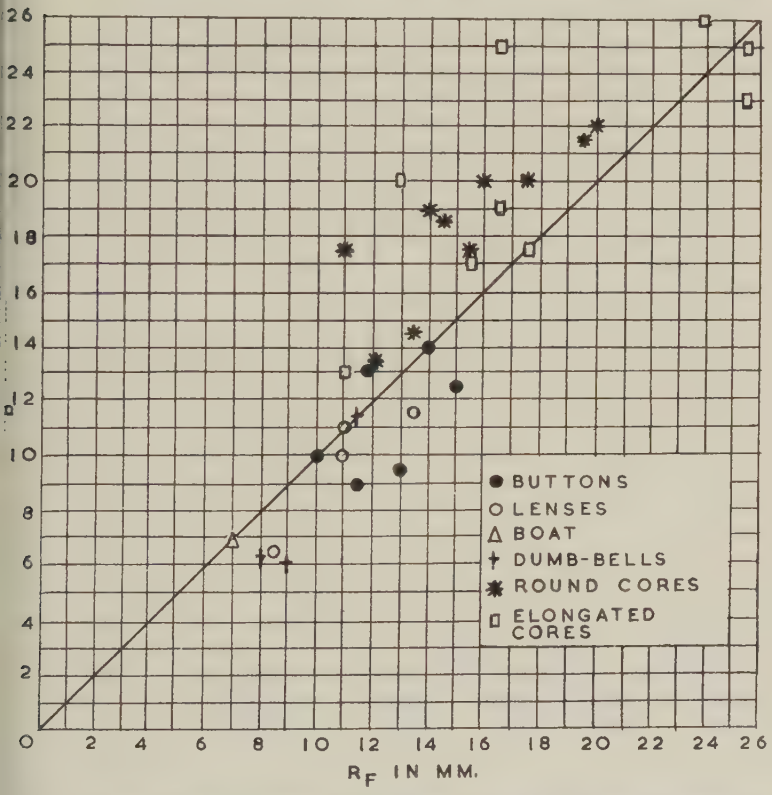

FIG. 2. Scatter diagram showing relationships of R_B and R_F values of australites from Harrow. (R_B and R_F radius of curvature of posterior and anterior surfaces respectively.)

cores were developed on ablation. Reduction of the primary forms, composed of relatively homogeneous tektite glass, to produce the secondary forms possessed by australites, evidently occurred during the atmospherical phase of earthward flight of these extra-terrestrial objects. For the production of sufficiently high temperatures leading to front surface ablation in progressive stages, primary forms of glass bodies are considered to have entered the earth's outer atmosphere as cold objects. All temperature and pressure effects operating upon their

forwardly directed surfaces were generated by virtue of their traversing the atmosphere at very high velocities. Under such circumstances, the sculpturing of the anterior surfaces of australites and their reduction in volume by ablation can be explained in terms of gas dynamics at high speeds of flight.[1] Similar conditions were responsible for the shaping and sculpturing of the forward surfaces of the elongated australites (derived from original spheroids, ellipsoids, apioids, and dumb-bells of revolution).

Comparisons between the average specific gravity values and the average weights of complete specimens of australites from Harrow, with these properties for significant numbers of other south-west Victorian australites, are shown in table IV.

TABLE IV. Average specific gravity values and average weights of complete specimens from three australite concentration centres in south-western Victoria.

Concentration centre.	Average specific gravity.	Average weight (gm.) of complete specimens.
Harrow	2·42	8·97
Nirranda	2·41	2·56
Port Campbell ...	2·40	2·73

The average weight of complete specimens from Harrow is much greater than for Nirranda and Port Campbell, where larger numbers of the smaller button- and lens-shaped forms have been collected in proportion to the number of larger australite cores. At Harrow, which is the most westerly of these three concentration centres in the south-western Victoria strewnfield, the complete forms of australites are not only the heaviest, but they also possess the greater average specific gravity values. There is noted an increase in average specific gravity values from Port Campbell, the most easterly of these occurrences, through Nirranda to Harrow. Such a trend fits in well with the scheme of a provincial distribution of australites according to chemical composition across Australia, where, as a generality, and considering only those areas from which significant numbers of specimens have been collected, it is found that forms with the lower specific gravity occur in the east and forms with the higher specific gravity occur in the west of the continent.

Since the specific gravity of australite glass is related to its silica

[1] G. Baker, Nirranda strewnfield australites, southeast of Warrnambool, western Victoria. Mem. Nat. Mus. Victoria, 1954. (In press.)

content, the specific gravity increasing with decrease in silica content, it thus follows that the more acidic examples occur in the east and less acidic examples in the west, indicating a general chemical gradient across Australia.[1] In like manner, there is an increase in refractive index of natural glasses with decrease in silica. Tilley[2] has shown that the average specific refractivity of four australites (two from Mt. William in the Grampians, Victoria, and two from unknown localities) is 0·2109. The average for the two Mt. William specimens is 0·2117, and that for two australites from Harrow has been determined as 0·2109 from the formula $K = (n-1)/d$, where K is the specific refractivity, n the refractive index of the australite glass, and d its specific gravity or density. Tilley found that a graphical plot of density and specific refractivity (K) relations was broken up into fields separating tektites generally from terrestrial volcanic glasses, thus confirming divergences of the properties of tektites from those of terrestrial glasses of natural origin, and lending support to the theory of the extra-terrestrial origin of tektite glass. The specific refractivities of the two Harrow examples are given in table V for comparison with those determined by Tilley (1922) for the Mt. William australites.

TABLE V. Specific gravity, refractive index, and specific refractivity comparisons between australites from Harrow and Mt. William.

Locality.	Specific gravity.	n_{Na}.	K.	Author.
Mt. William, Victoria	2·393	1·504	0·2106	Tilley (1922)
,, ,,	2·443	1·520	0·2128	,, ,,
Harrow, Victoria	2·431	1·512	0·2103	Baker (this paper)
,, ,,	2·446	1·517	0·2114	,, ,,

The first example from Harrow is a button-shaped australite, the second is an elongated core (possibly originally a boat-shaped form). These are numbers 5 and 28 respectively in table I.

[1] G. Baker and H. C. Forster, The specific gravity relationships of australites. Amer. Journ. Sci., 1943, vol. 241, pp. 377–406. [M.A. 9–303.]

[2] C. E. Tilley, Density, refractivity, and composition relations of some natural glasses. Min. Mag., 1922, vol. 19, pp. 275–294.

Dehydration of the montmorillonite minerals.

By R. Greene-Kelly, B.Sc., Ph.D.

Rothamsted Experimental Station, Harpenden, Herts.

[Taken as read January 27, 1955.]

Introduction.

STUDIES of the effect of dehydration at temperatures greater than 150° on sorption by montmorillonites have shown that small interlayer cations such as lithium and magnesium promote an irreversible decrease in the amount of interlamellar sorption and a consequent marked fall in the cation exchange capacity as measured by conventional methods (1, 2, 3, 4). The other minerals of the group do not show this property (4), which is quite distinct from the supposed 'potassium fixation' reported in these minerals (5). This latter effect, which is small for montmorillonite, refers to the decreased rate of exchange of potassium as compared with smaller exchange cations especially after the potassium-saturated mineral has been dried at 100° C., and has been shown to be much more marked in mica-like minerals with silicate layers of higher charge density (e.g. illites and vermiculites (6)). The amount of water sorbed by potassium-saturated montmorillonite is not significantly affected by drying at temperatures below 400° C. although it is less than that of most other montmorillonites (3), due probably to the low hydration energy of the potassium ion (7).

In this paper the conditions leading to irreversible loss of internal surface are considered in greater detail. In the first part the susceptibility to irreversibility is considered for lithium-saturated minerals over the range of composition from montmorillonite to beidellite.[1] The end-members of this isomorphous series have been shown to differ markedly in their dehydration properties (4) and this has been made the basis for a simple test to distinguish them (8). Since, however, intermediate minerals exist, particularly in soils, it was thought desirable to investigate them also. The second part of this paper is concerned with the effect of only partly saturating the exchange complex of montmorillonite with lithium, the remaining ions being normal in their behaviour

[1] See appendix for remarks on the mineral 'beidellite'.

on dehydration. The effect on the internal surface of the two types of treatment is very similar, the difference being that in the first case the loss of surface is determined by the way the octahedral substitutions are distributed between silicate sheets, whereas in the second case it is determined by the way the two types of exchange cations spread themselves over the surface.

I. Montmorillonite-beidellite series.

Method.

The chief difficulty in carrying out this work was to find a number of analysed minerals whose unit cells have compositions intermediate between montmorillonite and beidellite. Unfortunately many of the samples that have been analysed were not pure and often no attempt had been made to distinguish between cations held superficially by the clay and those composing the silicate sheet. Foster (9) has emphasized the latter point with special reference to magnesium and found that several dioctahedral montmorillonite minerals formerly thought to have more than two out of the three octahedral positions filled with cations were actually nearly dioctahedral. Where silica, alumina, and iron oxides are closely associated with the clay mineral the problem of calculating the unit cell composition from total analyses is almost insoluble. Methods have been proposed whereby these impurities are selectively extracted by suitable reagents, and it has been shown that whereas the analyses indicated an unreasonable unit-cell composition, after correction not only was a reasonable unit-cell composition calculable but it often turned out to be nearly dioctahedral (10, 11). Such results increase confidence in selective solubility methods, but the necessity of relying on such empirical methods to arrive at unit-cell compositions can hardly be considered as satisfactory, since they require assumptions as to the amount of clay mineral attacked by the reagent.

The method used here to classify samples was based on the assumption that all the minerals investigated were strictly dioctahedral. The divalent cations not removed by repeated washing with ammonium acetate were assumed to originate from octahedral co-ordination in the clay mineral. Inspection of analyses given in the literature shows that magnesium is generally the only important divalent cation permissible in octahedral co-ordination.

The net charge was calculated from the exchange capacity. The justification for this procedure is that the samples were carefully selected,

purified by sedimentation, and examined by X-ray diffraction to avoid the possibility of contamination by non-expanding mica-like minerals. Analyses of the samples for potassium also served to confirm this point and provided a correction where necessary.

The percentage of the exchange capacity due to substitution of trivalent cations by magnesium was then taken as an index of the percentage of octahedral substitution. This method is admittedly an approximation, but in the light of present knowledge it is thought to give results which bear as much relation to the truth as the more conventional methods.

To carry out the dehydration tests the samples were first saturated with lithium, since lithium has been found to be the most active interlayer cation. The samples were then heated at various temperatures up to 300° C. and the loss of internal surface tested by taking X-ray diffraction photographs of the samples after treatment with glycerol. Glycerol was used because the X-ray photographs of glycerol-treated samples showed comparatively simple two-component random interstratification effects and because the relevant calculations had been carried out (12). The surface readily available to glycerol has been found to be roughly comparable to that available to water vapour.

Experimental procedure.

The samples suspected of containing a dioctahedral montmorillonite mineral were first submitted to a preliminary examination, which consisted of taking an X-ray photograph of the powder specimen treated with glycerol. About fifty samples containing a substantial proportion of a dioctahedral montmorillonite mineral were re-examined by saturating them with lithium, heating them to 200° C. overnight, and again testing their reaction with glycerol. The samples could be divided into three main groups, those that gave a rational 18° kX spacing, those giving a rational 9·5° kX spacing, and those showing considerable central scatter and an irrational sequence of 00*l* reflections. Representatives from each group were chosen and purified by dispersion to a 1 % suspension and passing through a Sharples supercentrifuge, the fraction less than 0·1 μ being retained. This fraction was concentrated by further centrifuging or by flocculation with calcium chloride. A little of the resultant gel was dried on a glass slide to provide oriented flakes and the remainder was washed with ammonium acetate until ammonium-saturated and then with alcohol until the excess ammonium acetate was removed.

The oriented flakes were cut from the glass slides, placed in small weighing bottles, and washed with 3N lithium chloride followed by alcohol until chloride-free. Samples of the flakes were heated at 100°, 150°, 200°, 250°, and 300° C., and soaked in glycerol at 80° C. overnight. X-ray photographs were taken with slit-collimated cylindrical cameras of 9 cm. diameter and filtered copper or cobalt radiation.

The exchange capacity of the samples was determined by distilling the ammonia in a semi-micro distillation apparatus after adding 2 ml. of 40 % sodium hydroxide. The exchange capacity thus determined compared favourably with that found by standard methods, and the results with duplication gave a reproducibility of ±3 m.e./100 gm. for an exchange capacity of 100 m.e./100 gm.

The analyses for magnesium, potassium, iron, and calcium were carried out on the ammonium-saturated sample by evaporating the sample in hydrofluoric acid and taking the residue up in nitric acid. The resultant solution was analysed for the elements mentioned using the Lundegärdh spectrographic method. An accuracy of about ±6 % of the amount present could be expected.

Results.

The results of analyses of the samples selected as representative of the montmorillonite-beidellite series are given in table I. Information concerning the source of samples is also included.

TABLE I. Chemical analyses and base-exchange capacity of the montmorillonite-beidellite series.

No.	Locality.	Exchange capacity m.e./100 gm.	Total analysis* in % K_2O,	Fe_2O_3,	MgO.	m.e./100 gm. of exchange capacity due to Mg.	% octahedral substitution.
1.	Black Jack mine, Idaho	94	0·2	0·7	0·16	4	4
2.	Plain of Akkar, Safita, Syria (IS17) ...	110	0·0	12·8	1·60	40	36
3.	Hathi-Ki-Dhani, India	73	0·0	7·6	1·20	30	41
4.	Unter-Rupsroth, Rhön	113	0·0	0·0	2·06	51	45
5.	Wyoming	89	0·0	4·4	2·48	62	70
6.	British Columbia ...	81	0·0	2·2	2·54	63	78
7.	Redhill, Surrey ...	82	0·0	7·4	2·78	70	85
8.	Elliots, Antigua ...	90	0·67	7·3	3·38	84	93†

* % CaO less than 0·1 %.

† Including 0·67 % K_2O in total charge, this value would reduce to 81 %.

Source of materials:

1, G. Nagelschmidt (14). 2, A. Muir. 3, Burmah Oil Co. 4, U. Hofmann. 5, F. W. Berk and Co., London. 6, Imperial Institute (no. Ca A 128). 7, Fullers Earth Union (no. XLCT). 8. Imperial Institute (no. L 158).

The X-ray results given in table II were interpreted by means of the spacing near 9 kX. It was concluded from the diffraction patterns that

the variations of spacing observed between samples was due to a tw
component randomly interstratified system: the components being ne
9·4 and 17·7 kX. This case has been investigated by Brown and Greer
Kelly (12), who calculated proportions of each component which wou
be required to produce a given sequence of basal reflections. The pro
portions 'p' of the 17·7 kX spacing were read off from fig. 2*a*[1] in the abo
paper after corrections had been applied to allow for small changes i
the 'c' values of the two components. The results are included i
table II.

TABLE II. Results of X-ray examination of the minerals after glycerol treatme
The interlayer spacing is given in kX, followed by 'p' proportion expanded.

No.	Untreated.	Heated 100°.	150°.	200°.	250°.	300° C.
1.	8·9 R	8·9 R	8·9 R	8·9 R	8·9 R	8·9 R
	1·0	1·0	1·0	1·0	1·0	1·0
2 (a).	8·9 R	8·9 R	8·9 R	9·0	9·0	9·1
	1·0	1·0	1·0	0·7	0·7	0·5
3 (b).	8·9 R	8·9 R	8·9 R	9·1	9·2	9·3
	1·0	1·0	1·0	0·5	0·3	0·2
4.	8·9 R	n. d.	9·0	9·1	9·1	9·2
	1·0	n. d.	0·7	0·5	0·5	0·3
5.	8·9 R	8·9 R	9·4 R	9·4 R	9·5 R	9·4 R
	1·0	1·0	0·0	0·0	0·0	0·0
6 (c).	8·9 R	8·9 R	9·2	9·6 R	9·6 R	9·6 R
	1·0	1·0	0·4	0·0	0·0	0·0
7.	8·9 R	8·9 R	9·0	9·4 R	9·4 R	9·4 R
	1·0	1·0	0·0	0·0	0·0	0·0
8.	8·9 R	8·9 R	9·2	9·4 R	9·4 R	9·4 R
	1·0	1·0	0·3	0·0	0·0	0·0

(a), Lines broad, few orders; a typical soil clay mineral. (b), Kaolinite presen
(c), Cristobalite present.
R, reflection is a member of rational 00*l* sequence. n.d. not determined.

In fig. 1 the percentages of octahedral substitution in the differe
minerals are plotted against the value of 'p' after heating the lithium
saturated mineral to 200° C. It can be seen that according to the co
ditions of the test, above 70 % octahedral substitution there is litt
expansion, but below this value there is a rise in 'p' reaching the hal
expanded state at about 40 45 % octahedral substitution. Unfort
nately it was not possible to obtain a beidellite containing about 20
octahedral substitution, but it seems likely that such a mineral would b
little affected b the treatment. Nontronites generally contain abou

[1] The ordinates in fig. 2*c* in reference 12 should read 2·95, 3·05, 3·15 kX instead
2·8, 3·0, and 3·2 kX.

0·8-1·0 % MgO and probably lie in the region 20-40 % octahedral substitution and their behaviour to the test is compatible with aforegoing results. Here again lack of sufficient amounts of samples of adequate purity did not permit detailed examination. It is noteworthy that of the fifty dioctahedral minerals investigated only five were not montmorillonites.

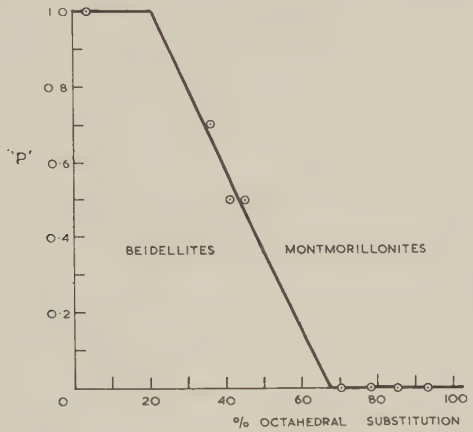

FIG. 1. Relation between the loss of internal surface after treatment and the percentage of octahedral substitution. Heating temperature 200° C.

Discussion.

Hofmann and Klemen (1) have suggested that the anomalous loss of expansion by lithium-montmorillonite after drying is due to the migration of lithium ions from the interlayer position to the vacant octahedral sites. They argue that this would tend to reduce the effective silicate sheet charge and make the mineral approach a non-expanding pyrophyllite-type structure.

Greene-Kelly (4) showed that only magnesium- and lithium-montmorillonite showed a marked dehydration hysteresis. This would be expected since the two ions are of the same size and would fit easily in the octahedral positions in the silicate sheet. Trioctahedral montmorillonite minerals were also shown to re-expand freely after lithium saturation and dehydration, and this is also to be expected, since no vacant octahedral sites are available for the migrating ions. Among the dioctahedral minerals, beidellites and nontronites were also found to be free from the hysteresis, and the results of this paper have shown that there is a correlation between the percentage of octahedral substitution and the

loss of expansion. These results could be explained if it were assumed that migration is only permissible when the silicate sheet charge is due to octahedral substitution. If all ions of the correct size migrate on dehydration then the effect on the expanding properties of the mineral will depend on the way the tetrahedral and octahedral substitutions occur in the mineral. If they occur so that all of one crystallite is tetrahedral and all of another octahedral, then after treatment there should be two sets of 00*l* reflections, one due to the expanded and the other due to unexpanded crystallites. On the other hand, if each crystallite consists of randomly interstratified silicate sheets each possessing only tetrahedral or octahedral charge, then the effect of the treatment will be to produce three concentrations of interlayer cations namely zero, half the normal number, and normal number of exchange cations per unit cell. Clearly the X-ray photograph of the glycerol-saturated specimen is liable to be complex, with the characteristic X-ray effects associated with random interstratification. The case where the silicate sheets are all similar in composition and contain both octahedral and tetrahedral substitution is interesting, since it will show the effect of decreasing the silicate sheet charge on the balance between the attractive force between the sheets and the repulsive force due to the sorption energy of the interlayer molecule. Random interstratification would not be expected in this case. It is probable that as the sheet charge decreases, the glycerol-treated mineral will show a sudden loss of expanding properties as the mineral approaches the pyrophyllite structure. In most of the cases studied there seems to have been random interstratification of 9·5 and 17·7 kX, and this suggests that there are differences in composition between the silicate sheets.

II. Lithium-sodium-montmorillonite.

Experimental procedure.

Pairs of 0·5 gm. samples of a purified montmorillonite from Redhill, Surrey, were washed five times with normal solutions of mixed lithium and sodium chlorides. They were washed free of chloride ions with alcohol-water mixtures and one of each pair was then heated to 200° C. The samples were washed with ammonium acetate, the washings being analysed spectrographically for lithium, sodium, and calcium. The samples were then freed from excess ammonium acetate with alcohol and analysed for ammonia. To determine the change of internal

surface, flakes containing known proportions of lithium and sodium were heated to 200° C. and the decrease of surface area determined by taking X-ray photographs of the glycerol-treated specimens as in part I.

Results.

Table III gives the results of the exchange capacity and X-ray measurements. It will be noticed that the calcium content is included with the

TABLE III. Relation between sodium introduced and sodium recovered after heating. The fraction, 'p', of the internal surface available to glycerol is also shown. (Exchange capacity of the unheated montmorillonite is 85 m.e./100 gm.)

m.e. ($Na^+ + Ca^{++}$) per 100 gm. introduced.	me. ($Na^+ + Ca^{++}$) per 100 gm. washed off after heating.	m.e. (Li^+) per 100 gm. washed off after heating.	'p'.
5	5	15	n. d.
15	8	11	n. d.
20	12	10	0·1
26	17	12	n. d.
27	20	12	0·25
48	29	15	1·0
57	45	16	1·0
70	65	6	1·0
79	74	5	1·0

n. d., not determined.

sodium content because of the difficulty of removing all the calcium from the exchange complex, and at low sodium values its contribution is appreciable. On the average about 3 milliequivalents of calcium per 100 gm. remained.

It will be seen that in general an appreciable amount of the sodium introduced was recovered after heating. The internal surface available to glycerol after heating is low at low sodium contents but rapidly increases to that of the fully expanding material when about 50 % of the exchange complex is sodium. All the heated samples still contained some exchangeable lithium: the lithium-saturated and heated mineral had a residual exchange capacity due to lithium of 15–20 m.e./100 gm. In fig. 2 the correlation of internal surface of heated samples with the exchange capacity measurements is made. It is interesting to note that X-ray photographs of heated lithium-sodium-montmorillonite treated with glycerol did not show any evidence of a 14 Å. reflection or its contribution to a mixed layer system.

Discussion.

When the amounts of inactive ions (sodium and calcium) were less than 50 % of the total exchange capacity, fig. 2 shows that about 65 % of the sodium and calcium introduced was recovered after the mineral had been heated. In this range of composition, the internal surface

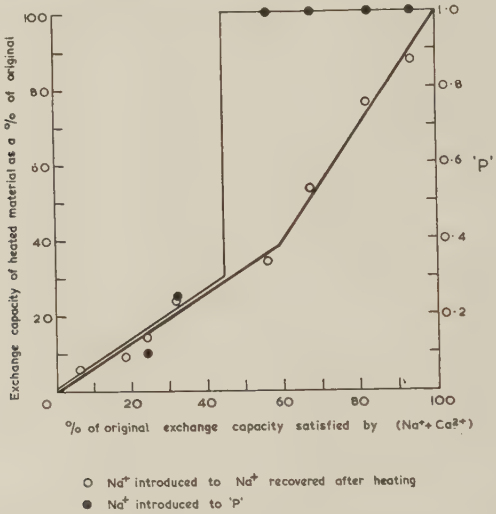

Fig. 2. Relation between the internal surface and exchangeable sodium available after treatment and the amount of sodium introduced. Heating temperature 200° C.

available to glycerol appeared to be comparable with the amount of sodium recovered. This suggests that the freely exchangeable sodium ions are concentrated in that part of the interlamellar space which is freely expanding. The remaining 35 % of the sodium introduced which is not freely exchangeable is presumably miscible with the lithium ions and consequently trapped when the latter migrate and the sheets are irreversibly brought together.

When the exchange complex contained above about 50 % sodium a marked change occurred. The X-ray results indicated that a high proportion of the internal surface became freely available to glycerol and at the same time there commenced an upward trend in the amount of sodium recovered. The composition of the fixed cations when this sudden expansion occurred was about 30 % sodium ions and the remainder lithium. It is interesting to note that when most of the surface

vas available to glycerol the amount of sodium recovered was still omewhat less than that introduced. This may be a reflection of the lightly different penetrating power of water and glycerol.

The fact that lithium-saturated and heated montmorillonites always ive some exchangeable lithium the amount of which appears to be ndependent of the composition of the mineral (for more than 70 % octahedral substitution) suggests that these cations are attached to sites external to the crystallites and these cations differ fundamentally from he interlamellar cations in their behaviour on dehydration. It is interesting to note that even if a high proportion of the sodium introduced is ecovered and the crystallites appear to expand fully with glycerol, the mount of lithium recovered is small. This suggests that these lithium ons are fixed even though the interlamellar surface is available and his would confirm the Hofmann and Klemen migration theory, since he lithium ions should be in octahedral sites. However, the lithium ons exchange freely at higher temperatures, because heated lithium-montmorillonite will exchange all the lithium in decinormal sodium hloride at 250° C. It is concluded, therefore, that the migration of the ithium ions occurs freely at 200–300° C., the direction of migration epending on the external conditions. This may be related to the instability of an ion which is too small for the co-ordination in which it inds itself. Migration to the octahedral sites satisfies both this requirement and that of being near the seat of charge in the silicate layer. The reverse migration is presumably due to the greater stability of a ydrated lithium ion in interlayer positions than that of an unhydrated ithium ion in octahedral co-ordination.

Conclusion.

The study of the two closely related systems, lithium-montmorillonite-beidellite and lithium-sodium-montmorillonite, has shown that neither system is a uniform one. In the former case it seems that there must be differences in composition between silicate sheets bound in the same crystallite, and in the latter case the majority of the sodium ions segregate to form a sodium-rich 'phase'.

The effect of heating on the internal surface available to glycerol of the lithium-saturated montmorillonite-beidellite is shown to be correlated with the amount of octahedral substitution; less than 70 % leading to some glycerol penetration. Likewise the study of the lithium-sodium-montmorillonite system indicated that, if there was less than

70 % lithium ions in the interlamellar spaces, expansion occurred after heating. No evidence of an intermediate state of expansion at 14 Å was found. The migration of the lithium ions on heating lithium saturated montmorillonites appears to explain fully all the experimental data.

Acknowledgements.—The author wishes to thank Mr. H. H. Le Rich for carrying out spectrographic analyses and also to thank the several donors of minerals mentioned in the text.

Appendix. A note on nomenclature.

Although montmorillonite is well established as a mineral, the somewhat rarer occurrences of beidellite had caused the existence of this mineral to be questioned (13). There is, however, little doubt that this mineral exists. Nagelschmidt discussed two beidellites (14), one of which was the type specimen from Beidell and the other a pure sample from Black Jack mine, Idaho. X-ray examination showed both samples were dioctahedral montmorillonites and the analytical results left no doubt that they should be classified as beidellites, since they were low in magnesium and ferrous iron. They contained only traces of potassium. The latter specimen has been used in this work and provides a nearly perfect end-member for the montmorillonite-beidellite series.

The results of Ross and Hendricks (15) have shown that the montmorillonite-beidellite series is probably continuous with no natural dividing boundary and have left the classification of the minerals of the series to be established arbitrarily. It is here suggested that it would be convenient if the term beidellite were reserved for those minerals with less than 50 % of their silicate sheet charge due to octahedral substitutions and montmorillonite for those in which it is more than 50 %. The term nontronite should be restricted to beidellite-type minerals high in iron and low in aluminium, and the term should not be used for possible nontronite-like minerals which derive most of their charge from octahedral substitutions and for which a new name should be proposed.

References.

1. Hofmann (U.) and Klemen (R.), 1950. Verlust der Austauschfähigkeit von Lithiumionen an Bentonit durch Erhitzung. Zeits. Anorg. Chem., vol. 262, pp. 95–99.

2. Greene-Kelly (R.), 1952. Irreversible dehydration in montmorillonite. Clay Minerals Bulletin, vol. 1, pp. 221–225.

3. Gonzalez Garcia (F.), 1950. Silicates del grupo de la montmorillonita. Anales de Edafología y Fisiología Vegetal, Madrid, vol. 9, p. 149.

4. Greene-Kelly (R.), 1953. Irreversible dehydration in montmorillonite, Part II. Clay Minerals Bulletin, vol. 2, pp. 52–56.

5. Raney (W. A.) and Hoover (C. D.), 1946. The release of artificially fixed potassium from kaolinite and montmorillonitic soils. Proc. Soil Sci. Soc. Amer., vol. 11, pp. 231–237.

6. Barshad (I.), 1948. Vermiculite and its relation to biotite as revealed by base exchange reactions, X-ray analysis, differential thermal curves, and water content. Amer. Min., vol. 33, pp. 655–678. [M.A. **10**–462.]

7. Norrish (K.), 1954. The swelling of montmorillonite. Discussion of Faraday Society on Flocculation (to be published).

8. Greene-Kelly (R.), 1953. The identification of montmorillonoids in clays. Journ. Soil Sci., vol. 4, pp. 233–237.

9. Foster (M. D.), 1951. The importance of exchangeable magnesium and cation-exchange capacity in the study of montmorillonitic clays. Amer. Min., vol. 36, pp. 717–730. [M.A. **11**–455.]

0. —— 1953. Geochemical studies of clay minerals III. Geochim. Cosmochim. Acta, vol. 3, pp. 143–154.

1. Earley (J. W.), Osthaus (B. B.), and Milne (I. H.), 1953. Purification and properties of montmorillonite. Amer. Min., vol. 38, pp. 707–724. [M.A. **12**–492.]

2. Brown (G.) and Greene-Kelly (R.), 1954. X-ray diffraction by a randomly interstratified clay mineral. Acta Cryst., vol. 7, pp. 101–103.

3. Pask (J. A.) and Davies (B.), 1945. Thermal analysis of clay minerals and acid extraction of alumina from clays. U.S. Bureau of Mines, Tech. Paper no. 664, pp. 56–81.

4. Nagelschmidt (G.), 1938. On the atomic arrangement and variability of the members of the montmorillonite group. Min. Mag., vol. 25, pp. 140–155.

5. Ross (C. S.) and Hendricks (S. B.), 1945. Minerals of the montmorillonite group: their origin and relation to soils and clays. Prof. Paper U.S. Geol. Surv., no. 205-B. [M.A. **10**–26.]